AD-A185 666 PROGRAM TO DEVELOPMENT AN OPTICAL TRANSISTOR AND SWITCH 1/1
(U) WESTINGHOUSE RESEARCH AND DEVELOPMENT CENTER
PITTSBURGH PA CR. T HENNINGSEN ET AL. 08 JUL 87
UNCLASSIFIED 87-9F4-NUTRN-R1 AFOSR-TR-87-1309 F/G 9/5 NL

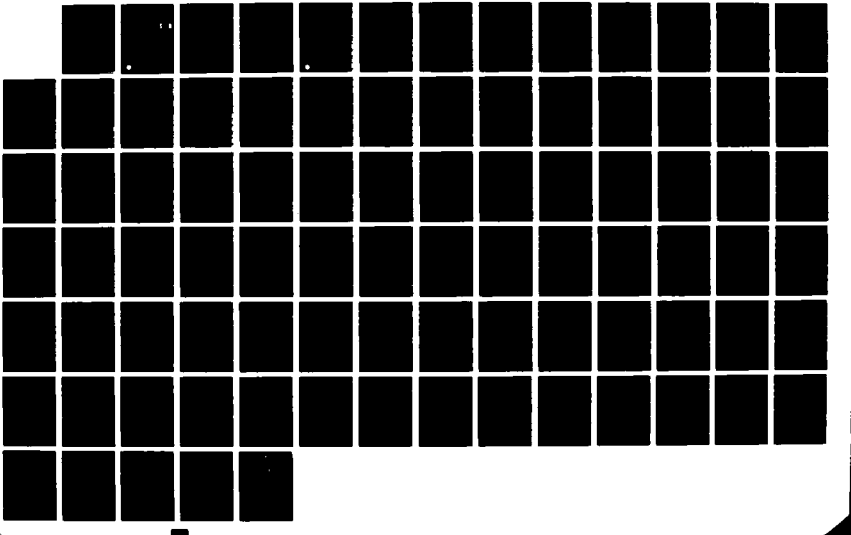

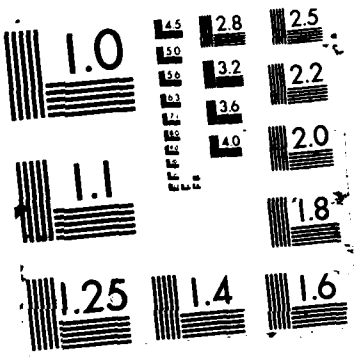
1.0
1.1
1.25
1.4
1.6
2.8
3.2
3.6
4.0
2.5
2.2
2.0
1.8

AFOSR-TR- 87-1309

PROGRAM TO DEVELOP AN OPTICAL TRANSISTOR AND SWITCH

T. Henningsen, M. Garbuny, and R. H. Hopkins
Crystal and Device Research Department

Final Report for the Period
September 1, 1984 to March 1, 1987

Contract No. F49620-84-C-0103DEF

Air Force Office of Scientific Research
Bolling AFB
Washington, DC 20332

July 8, 1987

Westinghouse R&D Center
1310 Beulah Road
Pittsburgh, Pennsylvania 15235

Unclassified
SECURITY CLASSIFICATION OF THIS PAGE

AD-A185 666

REPORT DOCUMENTATION PAGE

Form Approved
OMB No 0704-0188

1a REPORT SECURITY CLASSIFICATION Unclassified	1b RESTRICTIVE MARKINGS None
2a SECURITY CLASSIFICATION AUTHORITY -	3 DISTRIBUTION / AVAILABILITY OF REPORT Unlimited
2b DECLASSIFICATION / DOWNGRADING SCHEDULE -	
4 PERFORMING ORGANIZATION REPORT NUMBER(S) 87-9F4-NUTRN-R1 ✓	5 MONITORING ORGANIZATION REPORT NUMBER(S) AFOSR-TR- 87-1309
6a NAME OF PERFORMING ORGANIZATION Westinghouse R&D Center	6b OFFICE SYMBOL (If applicable) -
	7a NAME OF MONITORING ORGANIZATION - AFOSR
6c ADDRESS (City, State, and ZIP Code) 1310 Beulah Road Pittsburgh, PA 15235	7b ADDRESS (City, State, and ZIP Code) Bldg 410 Bolling AFB DC 20332-6448
8a NAME OF FUNDING / SPONSORING ORGANIZATION Air Force Office of Scientific Research	8b OFFICE SYMBOL (If applicable) NE
	9 PROCUREMENT INSTRUMENT IDENTIFICATION NUMBER F49620-84-C-0103
8c ADDRESS (City, State, and ZIP Code) Bolling AFB Washington, D.C. 20332	10 SOURCE OF FUNDING NUMBERS PROGRAM ELEMENT NO: 61102F; PROJECT NO: 2305; TASK NO: B4; WORK UNIT ACCESSION NO: -

11. TITLE (Include Security Classification)
Program to develop an optical transistor and switch

12 PERSONAL AUTHOR(S)
T. Henningsen, M. Garbuny, and R. H. Hopkins

13a TYPE OF REPORT	13b TIME COVERED	14 DATE OF REPORT (Year, Month, Day)	15 PAGE COUNT
FINAL	FROM 9-84 TO 3-87	July 8, 1987	77

16 SUPPLEMENTARY NOTATION
-

17 COSATI CODES			18 SUBJECT TERMS (Continue on reverse if necessary and identify by block number)
FIELD	GROUP	SUB-GROUP	optical. switch. transistors. absorption. rate. line. bands. relaxation. transition. photons. fluxes. singles. noise. materials. cross sections.

19 ABSTRACT (Continue on reverse if necessary and identify by block number)

The Optical Transistor and Switch, for which concepts and designs were developed under this program, is a device in which a radiation beam of one wavelength is controlled by a beam of a second wavelength. In contrast to other optical transistors and switches, this arrangement keeps the requirements for control and signal independent and thus adds another dimension to design. The basic device provides simply an optical path through a medium which consists of free three-energy level atoms such as sodium vapor at very low pressures. It provides, with relatively low optical powers, satisfactory switching action and transistor saturation gains of 3-10. A subsequent concept is that of Multistage Optical Transistors based on spectroscopically complementary materials. Very high transistor gains can be achieved with two variations of this concept. However, the higher optical power demand and the stringent requirement of double resonance between two materials are important drawbacks. The third concept is the Quantum Transition Etalon (QTE), which consists of a Fabry-Perot cavity enclosing the three-level medium. The QTE appears to have substantially the advantages of the two former concepts, but none of their limitations. With power demands typically 20-200 times lower than for the

20 DISTRIBUTION / AVAILABILITY OF ABSTRACT	21 ABSTRACT SECURITY CLASSIFICATION	
☒ UNCLASSIFIED/UNLIMITED ☒ SAME AS RPT ☐ DTIC USERS	Unclassified	
22a NAME OF RESPONSIBLE INDIVIDUAL R. H. Hopkins	22b TELEPHONE (Include Area Code) (412) 256-1341	22c OFFICE SYMBOL

DD Form 1473, JUN 86 Previous editions are obsolete

SECURITY CLASSIFICATION OF THIS PAGE
Unclassified

previous cases, the QTE achieves 40 dB in switching ratio and transistor gains that are, in principle, unlimited. This report includes updated versions of previous reports under this program, but places its major emphasis on the more recent studies on QTE design and operations.

PROGRAM TO DEVELOP AN OPTICAL TRANSISTOR AND SWITCH

T. Henningsen, M. Garbuny, and R. H. Hopkins
Crystal and Device Research Department

Final Report for the Period
September 1, 1984 to March 1, 1987

Contract No. F49620-84-C-0103DEF

Air Force Office of Scientific Research
Bolling AFB
Washington, DC 20332

July 8, 1987

Westinghouse R&D Center
1310 Beulah Road
Pittsburgh, Pennsylvania 15235

CONTENTS

LIST OF FIGURES

LIST OF TABLES

PROGRAM TO DEVELOP AN OPTICAL TRANSISTOR AND SWITCH

T. Henningsen, M. Garbuny, and R. H. Hopkins

ABSTRACT

The Optical Transistor and Switch, for which concepts and designs were developed under this program, is a device in which a radiation beam of one wavelength is controlled by a beam of a second wavelength. In contrast to other optical transistors and switches, this arrangement keeps the requirements for control and signal independent and thus adds another dimension to design. The basic device provides simply an optical path through a medium which consists of free three-energy level atoms such as sodium vapor at very low pressures. It provides, with relatively low optical powers, satisfactory switching action and transistor saturation gains of 3-10. A subsequent concept is that of Multistage Optical Transistors based on spectroscopically complementary materials. Very high transistor gains can be achieved with two variations of this concept. However, the higher optical power demand and the stringent requirement of double resonance between two materials are important drawbacks. The third concept is the Quantum Transition Etalon (QTE), which consists of a Fabry-Perot cavity enclosing the three-level medium. The QTE appears to have substantially the advantages of the two former concepts, but none of their limitations. With power demands typically 20-200 times lower than for the previous cases, the QTE achieves 40 dB in switching ratio and transistor gains that are, in principle, unlimited. This report includes updated versions of previous reports under this program, but places its major emphasis on the more recent studies on QTE design and operations.

1. INTRODUCTION, CONCLUSIONS AND RECOMENDATIONS

1.1 INTRODUCTION

Optical transistors and switches have received considerable attention in the literature of the last decade.[1] All of this past work, at least to the extent searched and seen by us, deals with single-frequency devices. As a common feature, radiation at that frequency passes through an optically nonlinear medium within a Fabry-Perot etalon. The refractive index, or the absorption, of the medium is then a function of the radiation intensity in the nonlinear domain so that different resonance conditions of the etalon can be realized, resulting usually in bistable operation.

The objective of the present program is the development of an optical transistor and switch which is much closer related to the Quantum Counter.[2] This type of device, first described and demonstrated for switching with uranyl by T. A. Gould and T. Henningsen,[3] applies two beams of different frequencies interacting with three levels of an atomic or molecular system.

The present program on an optical transistor and switch appeared in the beginning to require mainly the development of a mathematical model dealing with the complex interaction of two light beams in a three-energy level atomic system and to select, and ultimately test, materials accordingly. In the actual pursuit of this program, however, it soon became apparent that the problems to be dealt with lay elsewhere. First, it turned out that there exist materials, such as the vapors of alkali metals, which, in terms of their ideal performance, could be expected to outclass all other possible materials. Second, the interaction processes in these materials were in fact simple enough to obviate the necessity of creating a mathematical computer-assisted

program for their solution. Standard rate equations yielded these solutions readily. Third, after these solutions were obtained, it became clear that even optimal materials yield transistor gains not exceeding 12. For many applications, far higher gains will be required.

Thus, it became necessary to investigate extensions of the basic three-level interaction process. Much of this has been described in the three previous reports under this project, but an updated account of these developments is presented in Chapters 2, 3, and 4. It is concluded that, in many respects, the third concept, called the Quantum Transition Etalon (QTE), represents the most attractive solution since it combines very high gains with the lowest demands on material and optical powers. Section 5 represents the most recent work, viz., the analysis of the alternatives of operations which are possible with the QTE.

1.2 CONCLUSIONS AND RECOMMENDATIONS

The two-year program on the development of an Optical Transistor and Switch has generated and theoretically evaluated a series of concepts that evolved from the original basic idea to quite different embodiments. The original concept provides the basis for the successive developments. It is, quite simply, a three-energy level atomic system exemplified by sodium or lithium, applied in practice in exceedingly small amounts as integrated optical circuit elements. Two sources of optical radiation are used with different frequencies in the visible or infrared region. The first, providing the control beam, produces a population in the intermediate atomic level by excitation from the ground state. The second source generates the signal beam with a frequency at which transitions between the intermediate level and the third level provide absorption or stimulated emission. The control beam, then, can either operate as a switch turning the signal beam off and on, or as a transistor, modulating the signal power (with negative gain, i.e., the sign of signal increments is opposite to that of the control power increments). If lithium is used, switching by 30 dB requires 63 μW of control power for a 40 μm diameter fiber (i.e.,

5.0 W/cm^2); sodium yields the same performance with 25 μW (2.0 W/cm^2). In transistor operation, saturation gains in the limit of large incident signal power are 11.9 for lithium and 3.5 for sodium, but 110 μW and 13 μW are required, respectively, to reach half these gains. This gain behavior cannot be much improved by selecting other materials, since the pertinent energy exchange processes appear to be already optimal in the alkali metals. It was necessary, therefore, to search for innovative schemes to attain larger transistor gains. One such improvement was the concept of multi-stage optical transistors based on two materials with spectroscopically complementary energy levels. In this scheme, the output signal of one material serves as the control power of the other. Very high total gains can be obtained with either of two alternatives, viz., (1) a chain of discrete complementary transistor units, or (2) a monolithic mixture of complementary transistor materials (a concept which has no electronic analog). The condition of complementarity is that the frequency of one beam must excite level transitions 1→2 of one material and 2→3 of the other, with a corresponding match for the other frequency.

This condition, which cannot be met, e.g., with the sharp line structure of the alkali metals, is far less stringent for the broader energy bands existing, especially, in the spectroscopy of solid state or semiconductor materials. Although with such bands the gain per stage (or per corresponding unit length of the continuum transistor) is reduced, that reduction is amply compensated by the exponential growth of the gain with the number of stages. A greater difficulty is posed by the need for constant photon fluxes which maintain the bias level for control and signal. The resulting optical power demand grows only linearly with the length of the transistor chain but, in the solid state materials considered, radiationless (phonon-assisted) transitions exact a relatively high toll in power.

The combination of high gain with relatively low optical power demand required a third concept, viz., the introduction of the three-level medium into a Fabry-Perot cavity resonant at the signal frequency. In the basic single-pass transistor, the gain approaches saturation only

for sufficiently large powers of the incident signal. It is clear that the demand on signal power is reduced by orders of magnitude if the signal undergoes a large number of passes through an optical cavity. Indeed the analysis shows that single-pass saturation gains are obtained for (by comparison) much smaller signal powers in etalon operation at correspondingly small control powers. However, as the control power increases, a complex interaction develops between the partially bleached medium and the characteristics of a lossy etalon. This shows itself in the appearance of a reflected signal beam, which grows at the expense of transmission, and in gains (of opposite sign for transmission and reflection) which can be used, in principle, at arbitrarily large values. There exist the following two classes (or modes) of operation.

In Class I, which is particularly suitable for small incident signals, the output powers of transmission and reflection are single-valued functions of the control power. Thus, transmission has a negative, and reflection a positive, gain over the entire range of power; but there exists for each curve a region where the slopes go through a point of inflection and where the (negative or positive) gains can be made arbitrarily large. If one keeps the control power, including its programmed excursions (and fluctuations), within a selected interval around the inflection point, the gain can be held constant within prescribed limits. However, the allowed size of the interval is inversely proportional to the gain. Since gains above 103 appear to be feasible, Class I characteristics are particularly suitable for the transistor amplification of small optical signals. A signal bias power of about 1 μW ($\simeq$ 0.1 W/cm^2) and control bias power of about 0.3 μW are typically required for beams of 40 μm diameter. These are considerably smaller power demands than even those of the basic transistor device.

Class II can be characterized by its bistability between two branches of operation. As the control power is varied from zero up to, and beyond, a certain critical (apex) value, the transmission of a fixed incident signal proceeds on a branch of relatively high transparency and at the critical value abruptly drops to a second branch of high opacity.

The return of the control power to zero on this second branch follows a hysteresis loop; i.e., at a second, lower, critical value, the transmission abruptly rises to the first branch. Meanwhile, reflection behaves in a complementary manner. Class II, therefore, is most suitable for the operation of an optical switch (which is "normally on"). Switching signal power, e.g., of 100 μW, from on to off by 40 dB requires from the control power source only a 10 μs pulse of about 20 μW, and sustaining power of 3 μW. In the examples previously given, the transitions between branches can occur within less than a nanosecond.

2. THE ELEMENTARY SWITCH AND TRANSISTOR UNIT

2.1 MATERIALS SELECTION FOR OPTICAL SWITCHES AND TRANSISTORS

The basic concept of optical switches and transistors (OST) is rather simple (see Figure 1). Two beams enter the device.[3] The first, called the control (or pump), acts by inducing absorption on the second, called the signal. As a switch, the control turns the signal on or off (i.e., by reducing it to an acceptable level, such as 10^{-3}, of the initial intensity). In transistor operation, a small variation of the control produces a large variation of the signal, thereby amplifying alternating optical power. Alternatively, the transistor is actually a quantum counter[2] transferring power from one frequency to another more desirable, e.g., for detection. In the basic device, three atomic or molecular levels are involved. The frequency of the control beam is resonant with the transition between levels 1 and 2; hence, the population in level 2 is modulated by the control. The frequency of the signal beam is resonant with the transition between levels 2 and 3; hence the signal is passing or, more or less, absorbed, depending on the population in level 2, i.e., depending on the power of the control beam.

In principle, an almost unlimited number of materials and their spectroscopic energy terms could serve the purposes of OST. However, the number of eligible materials is drastically limited by many practical and inherent conditions. First, the frequencies of control and signal beams may be restricted by the user to certain more or less narrow intervals in the visible and infrared regions or the ultraviolet domain. Second, the OST devices must be designed as components of integrated optical circuitry. This does not imply necessarily that the materials themselves must form fibers or waveguides; they must, however,

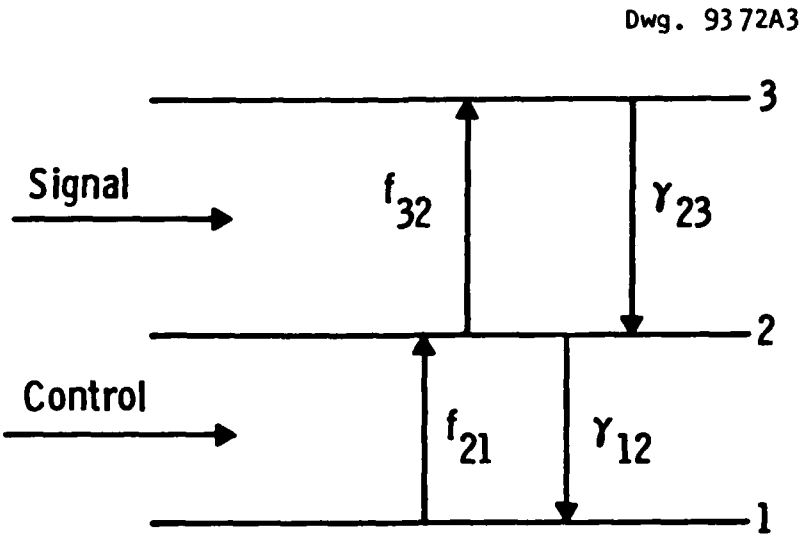

Figure 1. Schematic diagram of optical S&T operation.

be compatible with the design requirements of integrated optics, i.e., they must function with rather small active volumes. Third, the materials must operate passively, especially without the aid of remotely delivered electric power. Last but not least, certain stringent inherent conditions must be fulfilled by the energy levels of the material.

Level 2 must have a high relaxation rate,* γ_{12}, to the ground state (level 1), i.e., a short time constant, τ_{12}, to accommodate a high switching speed or large transistor bandwidth. On the other hand, the fraction of signal power transmitted is $\exp(-\sigma_{32}N_2L)$, where σ_{32} is the absorption cross section for the transition to level 3, N_2 the population density of level 2, and L the interaction length of the material. Thus, for a given control power, N_2 will be small for short time constants τ_{12}. Since L should also be small, sufficient leverage

*In this report we follow the convention of designating in γ_{12}, σ_{32}, etc., the first subindex as the final level, the second subindex as the initial level, of a transition.

for the control of the signal beam can only be obtained if σ_{32} is large. This represents a second condition for level 2. However, in the special case of an optical switch for which relatively long periods of bistable operation are desired, the conditions for level 2 can be considerably relaxed. A long lifetime of level 2 is in fact an advantage in this special case since it reduces the required control power.

Level 3 should have a relaxation rate $\gamma_{23} > \gamma_{12}$ so that an atom or molecule in level 2 can make many absorbing transitions to level 3 before it falls back to the ground state. A subsidiary condition for level 3 is that it have only negligible probability of relaxing into a state other than level 2 and, in particular, that $\gamma_{13} = 0$.

How do various materials fulfill the requirements stated in the foregoing? This question is of crucial importance for the further planning and procedure of this work. In the following, conclusions are summarized for the main classes of materials.

2.1.1 Condensed Matter (Solids and Liquids)

Solids, particularly if they can be constructed as fibers or waveguides, have the a-priori advantage that they lend themselves easily to use as integrated optics components. Liquids, such as dyes, share this advantage to some extent since they can be suspended in capillary fibers. Certain organic crystals and fibers also belong to the category of dense materials.

The dense matter state is characterized by the strong coupling that, in general, exists between the radiating or absorbing electric dipoles. This strong coupling entails broad bands (rather than lines) in the spectra with resulting low-absorption cross sections and radiative decay rates. Broad absorption bands have the advantage that they do not require highly frequency-selective power sources for excitation, but the disadvantage that such bands may overlap for control and signal levels. Initial analysis and experiments for the demonstration of the OST concept[3] were carried out on the example of UO_2^{2+} (uranyl). This solid has the following pertinent parameters[2,4]:

$$\sigma_{21}(460\ \text{nm}) = 1 \cdot 10^{-20}\text{cm}^2 \qquad \gamma_{12} = 0.00478 \cdot 10^{6}\text{sec}^{-1}$$
$$\sigma_{32}(460\ \text{nm}) = 0.36 \cdot 10^{-17}\text{cm}^2 \qquad \gamma_{23} = 2.5 \cdot 10^{6}\text{sec}^{-1}\ \text{(radiationless)}$$
$$\sigma_{31}(570\ \text{nm}) = 1.39 \cdot 10^{-17}\text{cm}^2 \qquad \gamma_{13} = 0.6 \cdot 10^{6}\text{sec}^{-1}$$

The experiments demonstrated optical switching action with a response time τ_{12} of about 200 μsec (= γ_{12}^{-1}), so that a switching rate up to a few kHz is possible. In dense materials excited states can relax by the relatively fast and radiationless energy transfer to phonons as seen for the rate γ_{23} in uranyl. This process here has the advantage of avoiding reradiation by spontaneous emission of the absorbed signal photons. Such reradiation has the effect of somewhat reducing the "net" absorption cross section σ_{32} at the signal frequency.

2.2 MOLECULAR GASES

A systematic study of candidate materials for OST operation has to include molecular gases because of the vast number of possible energy term schemes and transitions. Nevertheless, the application of molecular transitions to OST devices encounters several problems.

Electronic transitions in molecules are fast, but lie, for most gases, in a part of the ultraviolet region which is not likely to be of interest in OST applications or even compatible with integrated optics.

Vibrational transitions extend from wavelengths in the far infrared to wavelengths as short as 1.5 μm (if the first vibrational overtones are included). The near infrared region as such is not excluded from considerations since sources of sufficient power and detectors of sufficient sensitivity are available in this domain. Instead, the main problem lies in the long radiative lifetimes of excited vibrational levels, typically in the range of 10-50 msec. Collisional deexcitation to lower levels at suitable densities can increase the relaxation rates by orders of magnitude in a radiationless process not unlike the phonon transfer in solids. However, vibrational energy transfer by collisions affects all vibrational levels, although

not with the same cross sections. Whether this fact can be utilized to fulfill the level requirements stated before is a complex question.

2.3 FREE AND QUASI-FREE ATOM MEDIA

A third class of candidate materials is the state of free atoms, such as monatomic gases or the vapors of mercury and the alkali metals at low pressures. In these media, the electronic energy states of the atoms are, ideally, unperturbed by the fields of neighboring or colliding atoms. As a result, spontaneous emission and absorption lines have very narrow spectral widths, viz., in terms of the line frequency ν, typically a halfwidth $\Delta\nu_h^D \approx 10^{-6}\nu$ for Doppler broadening, and if the latter can be avoided, the natural width $\Delta\nu_h^N \sim 10^{-8}\ \nu$.

The free-atom state can be approximated by atoms that are weakly bound on substrates such as on the surface of a fiber (similar to the method of internal reflection spectroscopy) or the inside wall of a hollow fiber. Another approximation to the free-atom state are interstitial atoms or ions with unfilled d- or f-shells (such as the rare earths) in transparent host solids. Electronic transition within these shells is shielded from the fields of the surrounding host material environment and therefore yields sharp lines. Such media are called here "quasi-free atoms." Their line spectra are not as sharp as those of free atoms, but orders of magnitude narrower than those of the bands normally in solids.

In the following we use certain relationships of radiation theory for a comparison between free atoms and the other media in terms of the constants important for OST operation. These relationships have been used in the computation of the performance characteristics expected from the examples in Section 2.2.

2.3.1 Computation of Absorption Cross Sections and Radiative Decay Rates

Assume a medium with an absorption coefficient k_ν at the frequency ν. A beam of initial intensity $I_{\nu o}$ will then be attenuated to I_ν after passing through a length L of the medium:

$$I_\nu = I_{\nu o} e^{-k_\nu L} \tag{2-1}$$

For small values of the exponent, to which the case of the optical transistor can be reduced, Equation 2-1 becomes linear so that one obtains for the fraction of power absorbed from the initial power $P_{\nu o}$

$$P^A_\nu / P_{\nu o} = (1 - I_\nu / I_{\nu o}) \simeq k_\nu L;\ k_\nu L \ll 1 \tag{2-2}$$

The coefficient k_ν is a function of the frequency ν, described by the absorption line profile. The line may be narrow or broadened to a band. However, radiation theory makes a very general statement about the area under the profile, viz.,

$$\int k_\nu d\nu = (\pi e^2/mc)\ N f_{mn} = 0.0265\ f_{mn}\ N \tag{2-3}$$

where e and m are charge and mass of the electron, c the speed of light in vacuo, N the number density of atoms [cm^{-3}], and f_{mn} the <u>oscillator strength</u>* of the transition to a level m from a level n (see Figure 2). The numerical value in Equation 2-3 is computed for CGS units of all variables. It is seen that the absorption (coefficient) integral is independent of linewidth and frequency.

*The oscillator strength derives from the classical model of an electron oscillating around a positive charge for which the absorption integral in Equation 2-8 becomes simply $\pi e^2/mc$. In the actual quantised level structure of atoms, f_{mn} represents the factor by which any particular transition from n to m differs in strength from the classical model.

Dwg. 9372A36

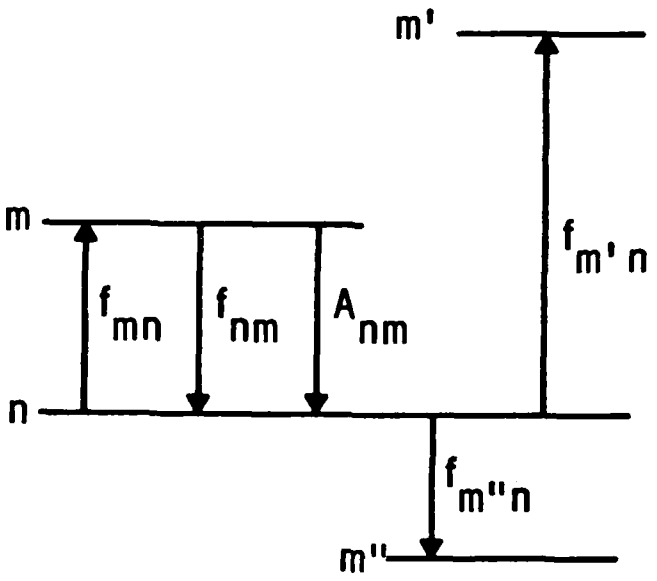

Figure 2. Designation of transition parameters.

To evaluate the absorption cross section from Equation 2-3, we transform the area under the absorption line profile into a rectangle of the line peak k_{max} as height and a linewidth $\Delta\nu$ as base so that

$$\int k_\nu d\nu \approx k_{max}\Delta\nu \qquad (2\text{-}4)$$

The cross section σ is then given by the relationship between absorption coefficient and absorber density, viz.,

$$k_{max} = N\sigma \qquad (2\text{-}5)$$

The absorption cross section follows thus from the last three equations as

$$\sigma = 0.0265\ f_{mn}/\Delta\nu \qquad (2\text{-}6)$$

The linewidth $\Delta\nu$ defined by Equation 2-4 will be of the same order of magnitude as the FWHM width, which is dependent on the line shape (e.g., Gaussian or Lorentzian).

Assuming an f-value of 0.1 and a linewidth $\Delta\nu = 1.10^{9}\text{sec}^{-1}$, one obtains from Equation 2-6 an absorption cross section $\sigma = 3.10^{-12}\text{cm}^{2}$. Such cross sections can be a factor of 10^{6}, or more, larger than those of the absorption bands in solids. Thus, in an OST device the population excited into level 2 by the control beam can be 10^{6} times smaller to achieve the same absorption as in a solid under otherwise equal conditions.

Of equal importance is the radiative decay rate (the Einstein spontaneous emission probability) A_{nm} ($= \gamma_{nm}$) from a level m to n (see Figure 2). From radiation theory,

$$A_{nm} = 8\pi^{2} \ (e^{2}/mc^{3}) \ \nu^{2} \ f_{nm} = 7.34 \cdot 10^{-22}\nu^{2}f_{nm} \qquad (2\text{-}7)$$

where f_{nm} is the oscillator strength of stimulated emission from (a higher) level m to a (lower) level n. Equation 2-7 has been derived for electronic dipole transitions in free atoms. It is not valid for radiationless decay or for other conditions governing the solid state.

Assuming a frequency $\nu = 4.10^{14}\text{sec}^{-1}$1 (corresponding to a wavelength of 740 nm) and again $f_{nm} = 0.1$, one obtains $A_{nm} = 1.2 \times 10^{7}\text{sec}^{-1}$. Thus, the speed of response in OST devices can be relatively high. Furthermore, the f-values chosen in the two previous examples are quite conservative and can usually be up to an order of magnitude larger for transitions between the first few levels above the ground state.

The f-values are implicit in measurements of either emission or absorption. The following relationship between the f-values for absorption and emission applies:

$$f_{nm} = - \ (g_{n}/g_{m}) \ f_{mn} \qquad (2\text{-}8)$$

where the g_n and g_m are the statistical weights of states n and m, respectively. The negative sign in Equation 2-8 results from the fact that the two f-values refer to energetically opposite effects, viz., one to absorption, the other to spontaneous emission. Equations 2-7 and 2-8 can be used to determine A_{nm}, f_{nm}, and f_{mn} from a measurement of either spontaneous emission intensity or absorption between levels n and m. This is important since published data are almost always based on only one type of measurement, usually emission.

Certain other considerations apply to the selection of suitable levels for optical transistor operation. It is seen from Equations 2-7 and 2-8 that, except for the g-values, the three constants A_{nm}, f_{nm}, and f_{mn} are proportional to each other. This proportionality, of course, does not extend to relationships between different transitions, such as between A_{nm} and $f_{m'n'}$ or $f_{m''n}$ (see Figure 2). Aside from different frequencies ν, f_{nm}, $f_{m'n'}$ and $f_{m''n}$ will be quite different. There exists, however, a condition of restraint in the f-sum rule:

$$\sum_m f_{mn} = z \tag{2-9}$$

where z is the number of electrons in the state n (usually equal to 1). As shown in Figure 2, this sum contains positive and negative values f_{mn}, corresponding to absorption and (stimulated) emission so that with Equation 2-8, one can also write for Equation 2-9

$$\sum_m f_{mn} = \sum_m \frac{g_m}{g_n} f_{nm} = z \tag{2-10}$$

where the first term on the left refers to absorption, the second to emission. The sums extend over all transitions from the level n which are permitted by the selection rules, although in emission the lower levels m may be in filled shells. The balance of f-values in Equation 2-10 makes it possible for OST operation to select a level 3

(see Figure 1) for which f_{23}, hence A_{23}, is appreciably larger than f_{12}, hence A_{12}. In this case, therefore, the radiative decay rates of levels 2 and 3 may fulfill the transistor condition stated at the start of this section.

In summary, we conclude that free atoms and, to some extent, quasi-free atoms offer absorption cross sections and radiative decay rates which are several orders of magnitude larger than those of other materials. As a result, fast response is possible coupled with minimal demand on the mass of active material and optical power. The analysis also predicts conditions for optical transistor gain; to this has to be added that parasitic (by-pass) transitions (such as those which give rise to a_{31} in the previous analysis[3]) can be easily avoided. Such media therefore deserve the first priority of theoretical and experimental investigation for OST devices.

2.4 PERFORMANCE EXPECTATIONS FOR OST DEVICES USING ALKALI METAL ATOMS

According to the preceding section, the materials of apparently greatest promise for OST operation are the media which consist of free atoms or, at least, contain quasi-free atoms. However, the choice must be limited to those elements (or their ions) for which the transition ν_{21} in the three-level system (level 1 always the atomic ground state) lies in a wavelength range compatible with restrictions of integrated optics. A survey of atomic line spectra reveals that there are two groups of media with elements fulfilling the wavelength condition. These are the metals in the first column of the periodic system, particularly the alkali atoms, and, second, transparent crystals or glasses which contain atoms or ions with unfilled shells such as the rare earths. The atoms of such media as the rare gases require excitation to level 2 in the far ultraviolet region, which is at present impossible, or at least extremely difficult, to match with the technology of integrated optics.

We have chosen to first investigate the performance of the alkali metals for several reasons. Spectroscopic f and A data are to a large extent available from tables,[6] although one has to derive, e.g., f_{mn}, from the experimentally determined f_{nm} with Equation 2-8. Thus, theoretical performance predictions for OST devices are possible with good accuracy. Subsequent verification by experiments with the vapor of alkali metals is not too difficult. Last but not least, the free-atom state may be approximated with quasi-free atom embodiments for practical devices.

The transition ν_{12} lies in the visible range for all alkali metals. The transitions to a level 3 have the feature that relaxation by radiation from level 3 to level 1 is forbidden by selection rules, i.e.,

$$\gamma_{13} = 0 \tag{2-11}$$

Thus, the coefficient a_{31}, which in the previous analysis[3] played an important complicating role, vanishes for these atoms:

$$a_{31} = \gamma_{13}/(\gamma_{13} + \gamma_{23}) = 0 \tag{2-12}$$

This fact simplifies all relationships starting with rate equations. We have thus for the absorbed pump power required to maintain an excited population density N_2 in level 2:

$$P_{abs} = n_2\gamma_{12}h\nu_{12} = LaN_2\gamma_{12}h\nu_{12} \tag{2-13}$$

where n_2 is the total population in level 2 contained in a volume of length L and cross-sectional area a. The application of Equation 2-13 to OST performance evaluation differs for switches and transistors.

2.4.1 Optical Switch

Here the objective is the bistable operation of signal power S between full transmission of a signal S and its attentuation by large factor, e.g., 30 db (10^3) to S_f:

$$S_f = S_o e^{-N_2 \sigma_{32}^{eff} L} \tag{2-14}$$

where the "effective absorption coefficient" σ_{32}^{eff} includes such effects as stimulated emission. The objective includes a low level of the required absorbed pump power and options of switching rates from zero to the highest possible value. Introduction of Equation 2-14 into Equation 2-13 yields for the necessary absorbed power:

$$P_{abs} = a \frac{\gamma_{12} h\nu_{12}}{\sigma_{32}^{eff}} \ln (S_o/S_f) \tag{2-15}$$

It is seen that the switching rate is limited by the radiative decay rate γ_{12} and the minimum power by that rate and the cross section σ_{32}.

2.4.2 Optical Transistor

Here we are concerned with changes of signal power S_f produced by a small change of the control power P_o around an operating point given by

$$P_{abs} = P_o (1 - e^{-N_1 \sigma_{21} L}) \tag{2-16}$$

and

$$S_f = S_o e^{-N_2 \sigma_{32} L} \tag{2-17}$$

A small variation of the control power P_o then produces, in first order, a linear change ΔP_{abs}. This produces a change ΔS_f in signal transmission of opposite sign.

The objective of the transistor is to maximize the gain G defined by

$$G = \left|\frac{\Delta S_f}{\Delta P_o}\right| \tag{2-18}$$

Here, with Equation 2-16

$$\frac{\Delta S_f}{\Delta P_o} = - \frac{\Delta S_{abs}}{\Delta P_{abs}} \left(1 - e^{-N_1 \sigma_{21} L}\right) \tag{2-19}$$

The mechanism of gain by "recirculation" of quanta has already been described for uranyl,[3] for radiationless decay from level 3 to level 2. We describe the process again for alkali metal spectra.

Each alkali atom which has been excited by the quantum $h\nu_{21}$ dwells in level 2 for a lifetime γ_{12}^{-1}. During this lifetime a number of quanta $h\nu_{32}$ may be absorbed by the atom from the signal power to level 3, which reradiates them at the rate γ_{23} spontaneously in random directions. Thus, there results for the absorption ratio:

$$\frac{\Delta S_{abs}}{\Delta P_{abs}} = \frac{\gamma_{23}\nu_{32}}{\gamma_{12}\nu_{21}} \tag{2-20}$$

Thus, one obtains with Equations 2-18 and 2-19 the gain

$$G = \frac{\gamma_{23}\nu_{32}}{\gamma_{12}\nu_{21}} \left(1 - e^{-N_1 \sigma_{21} L}\right) \tag{2-21}$$

The depletion of the control beam can be complete, i.e., the factor in Equation 2-21 contained in the bracket can approach unity, without bringing other limitations into play so that the gain approaches that given by Equation 2-20. This result obtained by partly intuitive reasoning is valid only for the special case that the statistical weights of levels 2 and 3 are equal. The following is a more rigorous treatment based on the pertinent rate equations.

An amount of control power, P_{abs}, absorbed in the device corresponds to $P_{abs}/h\nu_{12}$ photons absorbed. Similarly, the signal power S_o corresponds to $S_o/h\nu_{23}$ photons.

Under steady-state conditions the population densities N_2 and N_3 in levels 2 and 3 are constant. For level 2 we can, therefore, write

$$0 \equiv L\frac{dN_2}{dt} = \frac{P_{abs}}{ah\nu_{12}} - \gamma_{12} \cdot N_2 \cdot L + \gamma_{23}N_3 \cdot L - \sigma_{32} \cdot \frac{S_o}{ah\nu_{23}} \cdot \left(N_2 - \frac{g_2}{g_3} N_3\right)L \tag{2-22}$$

Here $P_{abs}/h\nu_{12}$ is, as described above, the number of photons absorbed from the control beam; $\gamma_{12}N_2L$ is the spontaneous decay of population N_2 with the time constant $1/\gamma_{12}$; $\gamma_{23}N_3 \cdot L$ is the radiative relaxation of population N_3; and $\gamma_{23}\, S_o/ah\nu_{23}\, (N_2 - g_2/g_3\, N_3)L$ is the balance of absorption and stimulated transitions between levels 2 and 3 caused by the signal beam S_o.

In the same way we find for level 3

$$0 \equiv L\frac{dN_3}{dt} = \sigma_{32} \cdot \frac{S_o}{ah\nu_{23}} \cdot \left(N_2 - \frac{g_2}{g_3} N_3\right) L - \gamma_{23}N_3 \cdot L \tag{2-23}$$

Equations 2-22 and 2-23 give

$$\frac{P_{abs}}{ah\nu_{12}} = L \cdot \gamma_{12} \cdot N_2 \tag{2-24}$$

From Equations 2-22, 2-23, and 2-24 we find the signal power S leaving the transistor after undergoing absorption caused by the control power P_{abs}

$$S = S_o - h\nu_{23} \cdot \frac{P_{abs}}{ah\nu_{12}} \frac{\frac{1}{\gamma_{12}}}{\frac{g_2}{g_3}\frac{1}{\gamma_{23}}} \frac{1}{1 + \frac{1}{\frac{g_2}{g_3}\frac{1}{\gamma_{23}}\sigma_{32} \cdot \frac{S_o}{ah\nu_{23}}}} \tag{2-25}$$

This calculation is valid for

$$S_o >> S_o - S,$$

i.e., for a small depletion of the signal beam. Similar results are obtained for higher depletions but the calculations are more complicated.

We define the amplification, G, in the optical transistor as the ratio between the change, ΔS, in the signal power S leaving the device to the corresponding change in the absorbed control power, ΔP_{abs}. From Equation 2-25 we have

$$G = \frac{\Delta S}{\Delta P_{abs}} = \frac{dS}{dP_{abs}} = G_f \times G_{ph} = \frac{\nu_{23}}{\nu_{12}} \times \frac{\gamma_{23} g_3}{\gamma_{12} g_2} \frac{1}{\frac{1}{1 + \frac{\sigma_{32} S_o}{ah\nu_{23}} \frac{g_2}{g_3} \frac{1}{\gamma_{23}}}} \tag{2-26}$$

Equation 2-26 can be written in the form

$$G = G_{sat} \left(\frac{1}{1 + S_h/S_o}\right) \tag{2-27}$$

where the saturation gain

$$G_{sat} = \left(\frac{\nu_{23}}{\nu_{12}}\right) \times \left(\frac{\gamma_{23} g_3}{\gamma_{12} g_2}\right) \tag{2-28}$$

is the maximum gain that can be obtained in a particular material. Furthermore,

$$S_h = ah\ \nu_{23} \left(\frac{g_3}{g_2}\right) \frac{\gamma_{23}}{\sigma_{32}} \qquad (2\text{-}29)$$

is the "half max gain" signal power, i.e., the signal power required to obtain half of the theoretical max gain, G_{max}, in the device. The smaller this number is, the less signal power is required to operate the device.

Figure 3 shows the nominal gain, $G(S_o)/G_{max}$ as a function of the signal power, S_o, which is normalized to the "half max gain" signal power S_h.

The numerical evaluations of the parameters important for OST, notably Equations 2-15 and 2-21, require a knowledge of the absorption cross sections and transition probabilities. These are directly available, or can be computed, from Tables published by the National Bureau of Standards.[6] The data are based on the intensities of the emission lines of 70 elements, limited, however, to the wavelength range from 200 to 900 nm. This material has been largely, although not completely, sufficient for the evaluation of the alkali metals. Necessary recalculations of these data were performed by using the relationships given in Section 2.1.

2.5 EXAMPLES

A choice of suitable atomic transitions is governed by the following principles:

(1) Level 1 is the ground state.

(2) For the switching device, according to Equation 2-15, $\gamma_{12}\nu_{12}/\sigma_{32}$ should be a minimum to keep the power demand for operation as small as possible. However, $\gamma_{12} = A_{12}$ should be large enough to fulfill the speed of response requirement. Hence, σ_{32} should be as large as possible.

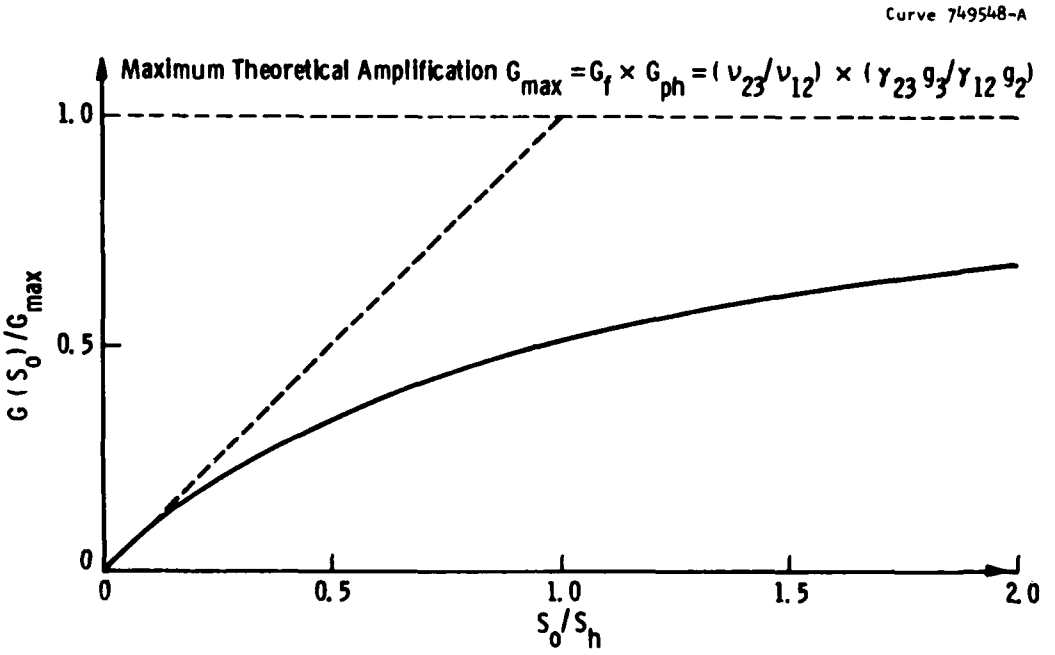

Figure 3. Normalized gain as a function of normalized signal power for a transistor.

(3) For the optical transistor, according to Equation 2-26 $(\gamma_{23}g_3\nu_{23}/\gamma_{12}g_2\nu_{12})$, which is the saturation gain of the device, should be as large as possible. The other parameters in Equation 2-26 determine how large the signal power S_o must be to reach the saturation gain within a few percent. In addition, the radiative decay rates should be large enough to meet the bandwidth requirements for the transistor.

The NBS tables[6] yield, for every measured emission line intensity, the values $g_n A_{nm}$ and $g_n f_{nm}$ ($m > n$ represents the upper level). The Einstein A_{nm} is here always equal to γ_{nm}. In lines with resolved fine structure, the statistical weight of a level equals $(2j+1)$. Where the tables report unresolved fine structure lines, the g-values correspond to the sum of the individual fine structure level g-values. The absorption oscillator strength f_{mn} follows from f_{nm} via

Equation 2-8. Equation 2-6 yields then the absorption cross section σ_{mn}. We adopted a model of alkali metal vapor at densities corresponding to pressures of 10^{-3} to 10^{-5} Torr. At such densities, the FWHM linewidth in sec^{-1} is given by the Doppler width

$$\Delta\nu_h = 7.17 \cdot 10^7 \nu \, (T/M')^{1/2} \qquad (2\text{-}29)$$

where T represents the temperature (K) and M'the molecular weight of the material.

2.5.1 Lithium

Figure 4 shows a diagram of energy term levels and transitions of lithium. As the first element of the second shell (ground state $1s^2 2s^2 S_{1/2}$), lithium has the feature that the lowest D-level is 3D (because of the quantum condition ($\ell \leq n-1$). This has the consequence that the transition 2P → 3D has several advantages for OST not present among the other alkali metals. The transitions selected for levels 1 → 2 and levels 2 → 3, respectively, are shown in bold arrows in Figure 4. The following are the data for the transitions and their levels.

The transition shown in Figure 4 of $3d\ ^2D_{3/2,5/2} \rightarrow 3p\ ^2P_{1/2,3/2}$ (in the far infrared) is expected to be quite weak and has been ignored.

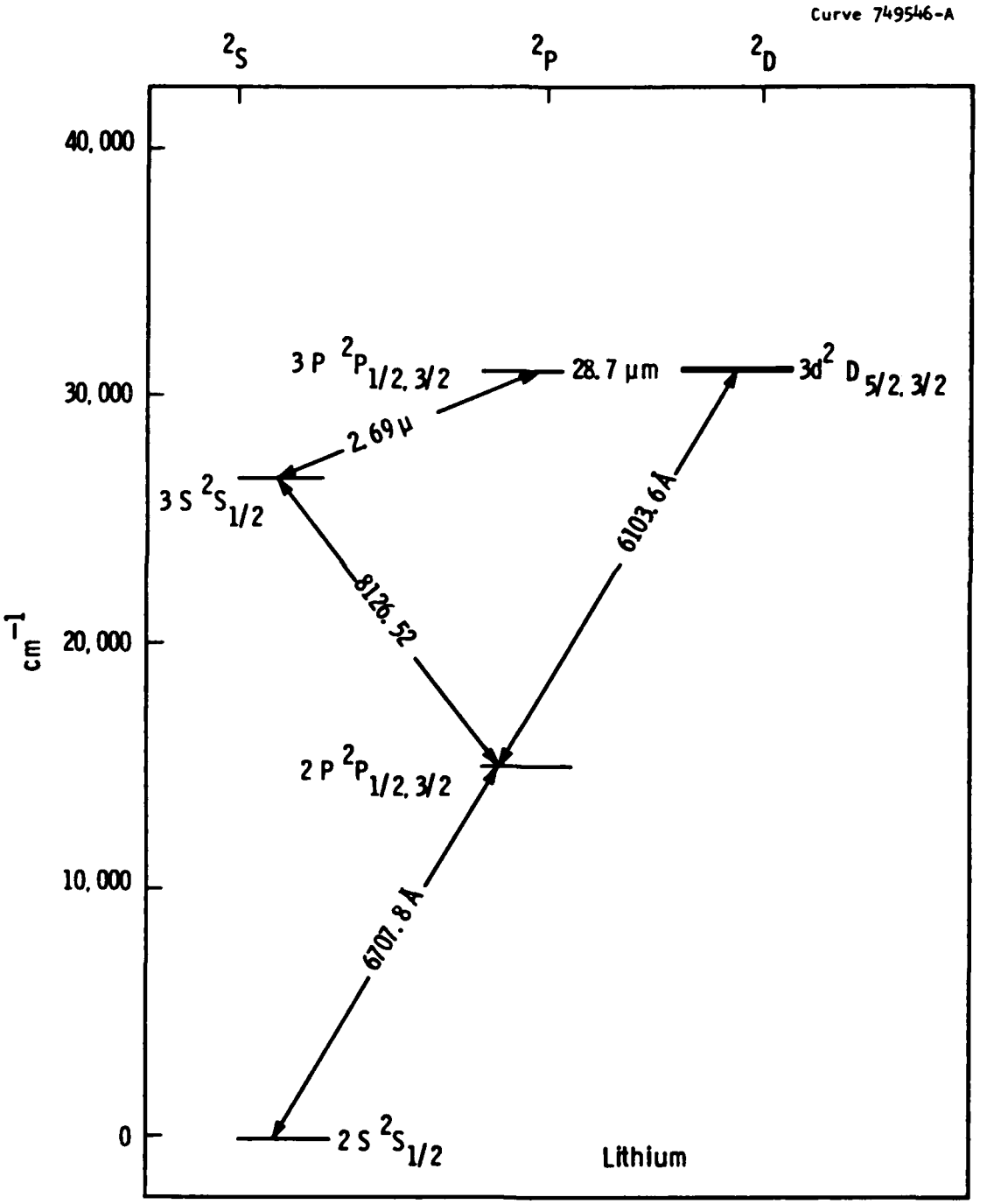

Figure 4. Lithium-spectrum.

Level 1	Level 2	Level 2	Level 3
$2s\ ^2S_{1/2} \rightarrow 2p\ ^2P_{1/2,32}$		$2p\ ^2P_{1/2,3/2} \rightarrow 3d\ ^2D_{3/2,5/2}$	
	$\lambda_{12} = 670.78$ nm		$\lambda_{23} = 610.36$ nm
	$\nu_{12} = 4.47 \cdot 10^{14} sec^{-1}$		$\nu_{23} = 4.91 \cdot 10^{14} sec^{-1}$
	$g_2 = 6,\ g_1 = 2$		$g_3 = 10,\ g_2 = 6$
	$g_2A_{12} = 1.2 \cdot 10^8 sec^{-1}$		$g_3A_{23} = 13 \cdot 10^8 sec^{-1}$
	$g_2f_{12} = 0.8$		$g_3f_{23} = 7.5$
$\gamma_{12} =$	$A_{12} = 0.2 \cdot 10^8 sec^{-1}$	$\gamma_{23} =$	$A_{23} = 1.3 \cdot 10^8 sec^{-1}$
	$f_{21} = 0.4$		$f_{32} = 1.25$
	$\Delta\nu_h = 4.14 \cdot 10^9 sec^{-1}$		$\Delta\nu_h = 4.55 \cdot 10^9 sec^{-1}$ (T = 500 K)
	$\sigma_{21} = 2.85 \cdot 10^{-12} cm^2$		$\sigma_{32} = 8.11 \cdot 10^{-12} cm^2$

2.5.1.1 Optical Switch

Using Equation 2-15 with $h = 6.63 \cdot 10^{-34}$ (Jsec), we have for the required control power density:

$$P_{abs}/a = 5.0\ W/cm^2 \tag{2-30}$$

or for the power P_o required for the cross-sectional area a of a 40 μm diameter fiber,

$$P_o = 64\ \mu W \tag{2-31}$$

This is the control power required to attenuate the signal power S_o to $S_f = 10^{-3}S_o$ (30 dB attenuation). The molecular density N_2, and the gas density N to be initially provided, follow from Equation 2-14:

$$N_2\ \sigma_{32}^{eff}\ L = \ln\ (S_o/S_f) = 6.9 \tag{2-32}$$

This yields for N_2L:

$$N_2L = 8.5 \cdot 10^{11} cm^{-2} \tag{2-33}$$

Allowing for the effect of stimulated emission from level 2 to level 1, we find that a gas density of

$$NL = 2.5 \cdot 10^{12} cm^{-2} \qquad (2\text{-}34)$$

is sufficient for steady-state conditions. Equation 2-34 corresponds to a pressure of 10^{-4} Torr for L = 1 cm length. The significance of Equation 2-34 is that, as shown by experimental and theoretical work,[7] metal atoms in the vapor phase at low pressures may fail to condense on selected substrates at normal temperatures. This is the case, even if the vapor pressure of the metal in bulk is much lower at that temperature than that of the metal atoms in the vapor phase.

The switching speed is determined by the slowest decay rate, viz., $A_{12} = 0.2 \cdot 10^{8} sec^{-1}$. The switching rate is therefore limited to 10 MHz, about 10^{3} times faster than uranyl.

2.5.1.2 Optical Transistor

According to Equation 2-27, the gain can be written in the form

$$G = G_{sat} \left(\frac{1}{1 + S_h/S_o} \right) \qquad (2\text{-}35)$$

With the data for lithium, the saturation gain G_{sat} equals

$$G_{sat} = \left(\frac{\gamma_{23} g_3}{\gamma_{12} g_2} \right) \cdot \left(\frac{\nu_{23}}{\nu_{12}} \right) = 10.8 \cdot 1.1 = 11.9 \qquad (2\text{-}36)$$

where we have separated the (saturation) photon multiplication and the photon energy gain factors, respectively. The signal power S_h (see Equation 2-27) required to reach $G_{sat}/2$ equals in flux density

$$S_h/a = 8.7 \ W/cm^2 \qquad (2\text{-}37)$$

so that for a 40 μm fiber

$$S_h = 110 \ \mu W \qquad (2\text{-}38)$$

The variation of the gain with S_o is thus

$$G = 11.9 \left(\frac{1}{1 + 110/S_o}\right) \qquad (2\text{-}39)$$

with S_o in μW. For S_o = 2200 μW, G reaches saturation within about 5%. Equation 2-39 is plotted in Figure 5.

2.5.2 Sodium

A procedure similar to that for lithium was adopted for sodium. In particular, analogous transitions between the levels were selected (see Figure 6). In sodium, the fine structure of level 2 is a doublet of sufficient spacing so that the NBS tables cite separately the transitions to and from the two sublevels, viz., 3p $^2P_{1/2}$ and 3p $^2P_{3/2}$. Nevertheless, the parameters important for OST operation are essentially the same numerically for both sublevels. A small advantage lies in the choice of the $^2P_{1/2}$ sublevel because of a slightly preferable frequency ratio and because (in the presence of stimulated emission from level 2 to level 1) its statistical weight, g = 2, requires fewer sodium atoms than the sublevel with g = 4. The important data of the selected transition are the following:

3s $^2S_{1/2}$ → 3p $^2P_{1/2}$

γ_{12} = 589.592 nm
$\nu_{12} = 5.08 \cdot 10^{14} \text{sec}^{-1}$
$A_{12} = 0.45 \cdot 10^{8} \text{sec}^{-1}$
$g_2 = g_3 = 2$

3p $^2P_{1/2}$ → 3d $^2D_{3/2,5/2}$

γ_{23} = 818.327 nm
$\nu_{23} = 3.67 \cdot 10^{14} \text{sec}^{-1}$
$A_{23} = 0.44 \cdot 10^{8} \text{sec}^{-1}$
$g_3 = 10, \; g_2 = 2$
$\sigma_{32} = 5.30 \cdot 10^{-11} \text{cm}^2$ (T = 500 K)

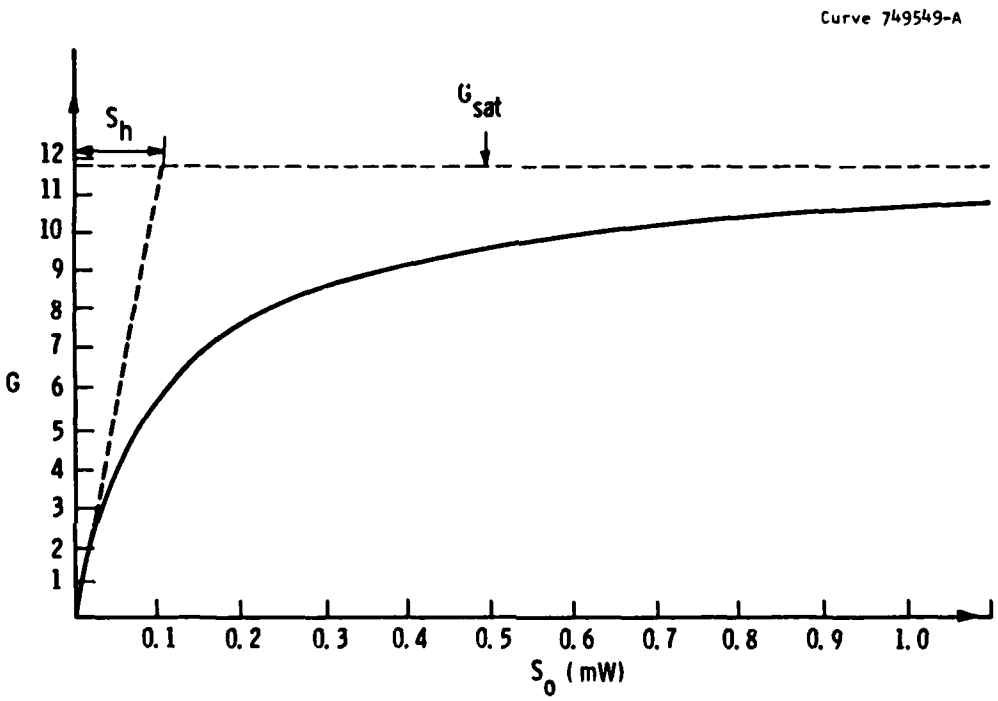

Figure 5. Gain in a lithium transistor.

2.5.2.1 Optical Switch

With calculations as in Section 2.5.1.1, one finds for 30 db attenuation

$$P_{abs}/a = 2.0 \text{ W/cm}^2 \qquad (2\text{-}40)$$

Control power in a 40 μm diameter fiber:

$$P_o = 25 \ \mu\text{W} \qquad (2\text{-}41)$$

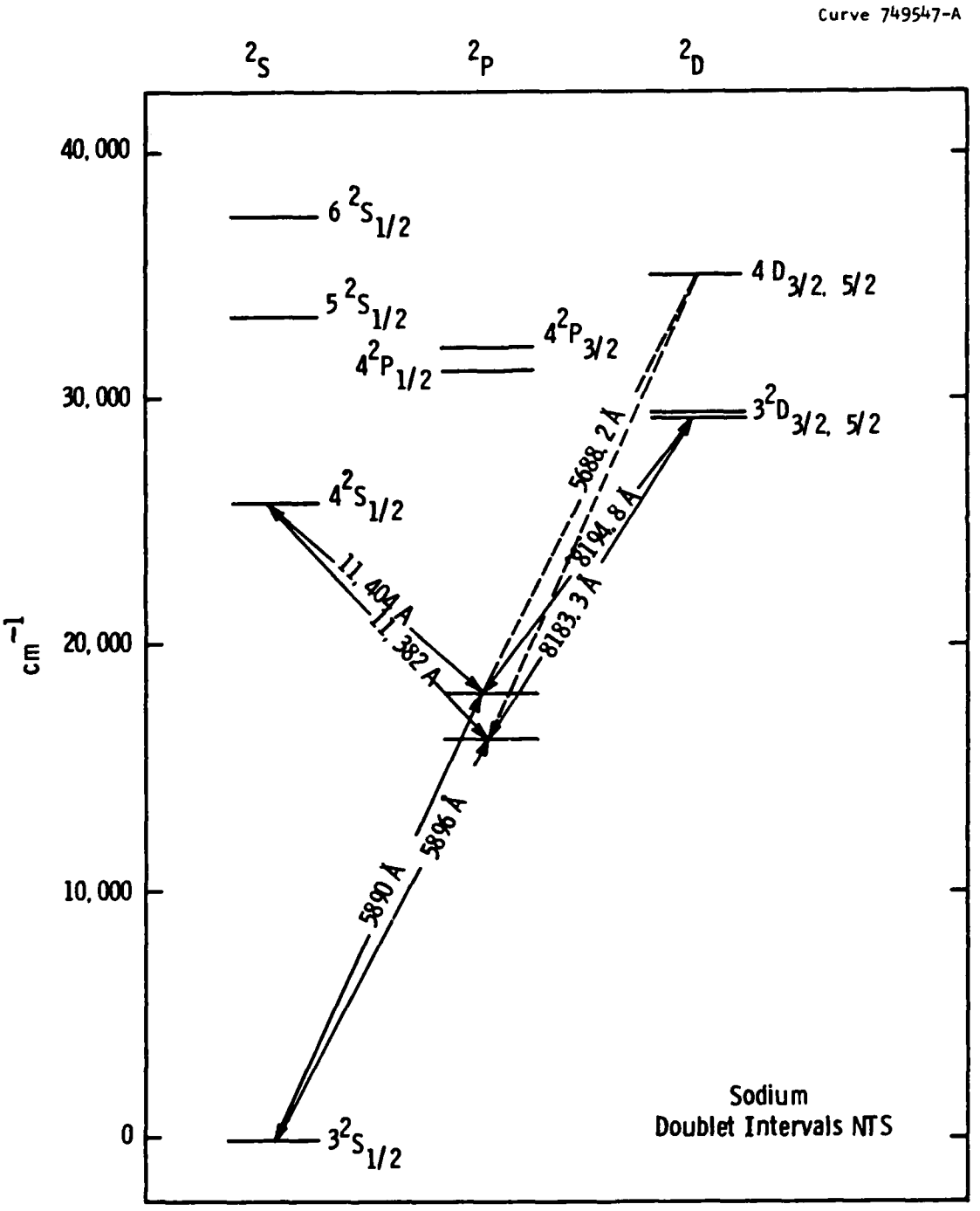

Figure 6. Sodium-spectrum.

Number of Na atoms required:

$$NL = 7 \cdot 10^{11} cm^{-2} \tag{2-42}$$

Limit of switching speed:

$$A_{23} = 0.44 \cdot 10^{8} sec^{-1} \tag{2-43}$$

Comparison with Equations 2-30 to 2-34 shows that sodium performs somewhat better as a switch than lithium. It requires less cut-off power, less material, and allows a switching rate of about 20 MHz.

2.5.2.2 Optical Transistor

The saturation gain, written as the product, respectively, of photon amplification and energy gain, is

$$G_{sat} = 4.89 \cdot 0.72 = 3.52 \tag{2-44}$$

The signal power required to reach half the saturation gain is

$$S_h/a = 1.00\ W/cm^2 \tag{2-45}$$

and for a 40 μm diameter fiber

$$S_h = 12.6\ \mu W \tag{2-46}$$

Thus, the results for the gain G as a function of the initial signal power S_o

$$G = 3.52 \left(\frac{1}{1 + 12.6/S_o}\right) \tag{2-47}$$

Comparing this result with Equation 2-39 for lithium, we conclude that although sodium has only 30% of the saturation gain of lithium, it approaches the saturation limit much faster. The two $G(S_o)$ curves of Equation 2-39 and 2-47 intersect at $G = 2.4$ with $S_o = 28\ \mu W$, below which sodium has the larger gain. Thus, the advantage of a lithium transistor comes into play only if larger signal powers are available.

3. CASCADED COMPLEMENTARY OPTICAL TRANSISTORS

3.1 BASIC UNIT OF COMPLEMENTARY OPTICAL TRANSISTORS

Section 2 dealt with single transistors and switches. Both devices are based on selected materials in which the essential energy structure consists of three levels excited by two beams: (1) the "control" beam, which excites the intermediate level 2 by resonance absorption from the ground state 1; and (2) the (then called) "signal" beam which is partially, or (in switches) completely, absorbed by the excited population of level 2 in transistors to the level 3. In the case of transistor operation, materials and power levels are chosen in such a way that the dynamic (ac) gain is maximized. It was shown that such gain may reach values of up to nearly 12 in the alkali metal vapors.

Figure 7 shows the energy term schemes of two transistor materials (I and II) which are complementary to each other. By this is meant that the energy difference of levels 1 and 2 in the first transistor is equal to that of levels 2 and 3 of the second transistor; similarly, the energy difference between levels 2 and 3 of the first equals that between levels 1 and 2 of the second transistor. Although drawn separately, transistors I and II are in good optical contact, i.e., radiation passes from one to the other with negligible loss. Thus, as depicted in Figure 7, a control beam A excites transitions from the ground state to level 2 in the first in transistor I, but the portion of beam A not absorbed in this process excites transitions of a population in level 2 of transistor II to level 3. This population is generated by a beam B which, in analogy to electronic transistor nomenclature, we now call the "collector" beam (replacing the previous term "signal"). The collector beam undergoes a process complementary to

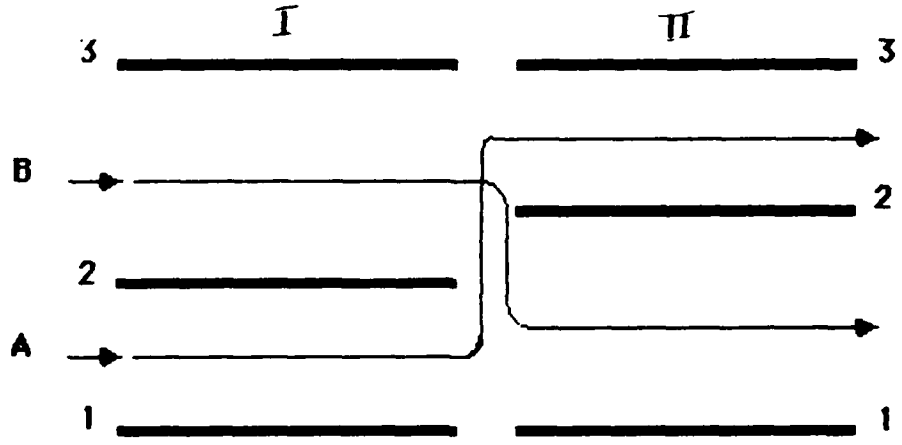

Figure 7. Basic unit of complementary optical transistors.

that of the control beam, i.e., it excites transitions 2-3 in I and 1-2 in II. The assembly of two transistors as just described may be considered as a basic complementary optical transistor unit within a transistor chain. However, as will be seen in the following discussion, in general it is necessary to add (to what is shown in Figure 7) a network of constant radiation power to maintain the gain of the alternating radiation signal.

3.1.1 Gain Considerations of the Complementary Unit as First Stage

Assume a small signal ΔA (in number of photons) is introduced into the first transistor (I) as control power (see Figure 8). The fraction of ΔA absorbed by transitions from level 1 to level 2 can be adjusted, of course, by a choice of the transistor path length L' or by the density of the absorption centers. Figure 8 indicates the important, and mathematically convenient, case that ΔA is completely absorbed. A collector beam B_1 of sufficient power is provided to achieve a gain G' in the number of transitions from level 1 to level 2. Thus, beam B_1 loses $G' \Delta A$ photons by multiple absorptions and becomes the control beam of strength $(B_1 - G' \Delta A)$ for the complementary transistor (II). On the other

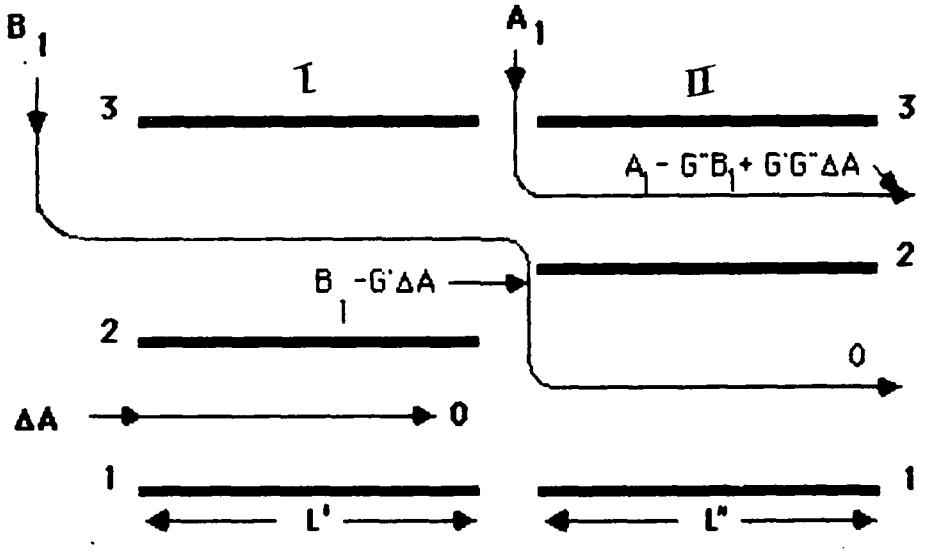

Figure 8. Gain operation of complementary transistor unit.

hand, beam ΔA, completely absorbed in transistor I, has nothing to contribute to transistor II. Thus, a collector current A_1 has to be supplied in sufficient strength for the transitions between level 2 and 3 in transistor II. Here again the path length L" is adjusted for complete absorption of the control beam, resulting in a gain G" for transistor II. G" thus serves as multiplier for the power (B_1-G'ΔA) so that the collector beam A_1 emerges from the complementary optical transistor unit with the power

$$A = A_1 - G''B_1 + G'G''\Delta A. \qquad (3\text{-}1)$$

The first two terms on the right of Equation 3-1 represent constant (dc) power supply contributions. The third term, however, represents the alternating (ac) signal ΔA multiplied by a gain G where

$$G = G'G''. \qquad (3\text{-}2)$$

These considerations show that the two complementary transistors operate synergistically; the original signal photons are reproduced with the gain given by Equation 3-2. Furthermore, multiple complementary units can be arranged in cascade resulting in an exponential increase of total gain, as will be discussed in a later section in greater detail. The capability of exponential gain is of particular importance for the choice of materials. Such gain requires, at least in principle, only that $G > 1$, even if either G'or G" is smaller than unity.

3.1.2 Search for Suitable Complementary Transistor Materials

Given a material of very narrow absorption lines for one of the transistors, the probability of finding a complementary transistor material is sharply decreasing if one expects it to approach a similar linewidth. On the other hand, the prospects for matching energy levels are much improved provided one is content with broader widths for the spectrum of the second material. Even materials exhibiting partly overlapping spectral quasi-continua can have transistor gains larger than unity as has been projected,[3] e.g., for uranyl.

Concurrently, we are in the process of searching among the spectra of rare earths (Types 4f and 5f) in various host materials for suitable candidates of a mutual match. This search presents a prolonged task since the pertinent data must be gathered from individual publications rather than from table collections as they are available for spectra of free atoms.[4]

3.2 DISCRETE COMPLEMENTARY UNITS IN OPTICAL TRANSISTOR CHAIN

The construction of a transistor chain of discrete units, such as shown in Figure 8, requires the periodic injection of dc optical power to maintain transitions between levels 2 and 3 for each transistor for sufficient absorption gain. Such optical systems are analogous to the Darlington circuits of electronic transistor amplifiers in which the emitter current of stage n becomes the base current for stage (n+1),

while for each stage a dc input ("collector") flux must be provided. In the optical case under discussion, of course, the dc supply radiation for material I must have the frequency of B_1 and, alternatively, for material II that of A_1.

Thus, it is necessary to inject successively B_1, A_1, B_2, A_2, B_3, A_3, B_n, A_n for n complementary units. To determine the size of these dc components, it is permissible (in small-signal theory) to ignore the effect of the ac components, but it must be considered that the relatively large dc components also undergo amplification. This is shown in Figure 8 for the first stage. Beam B_1, which maintains the gain in the first transistor and is then injected as control into the second detector, reduces the collector beam A_1 by the amplified amount of absorption $(-)G''B_1$. The reduction may severely depress gain G", unles A_1 is made large enough to compensate for this loss.

The relationship between gain and the collector beam power is shown in Figure 3. It will be seen that the gain as a function of the collector flux input S_o equals

$$G = G_{sat} \ (1 + S_h/S_o)^{-1}, \qquad (3\text{-}3)$$

where S_h is the flux input at which G reaches $G_{sat}/2$, i.e., half the gain saturation. Thus, the gain rises at first relatively fast before it approaches saturation asymptotically. In the following calculations we will, for convenience, assume dc fluxes high enough so that variations of the gain due to the absorption process can be ignored, i.e., G'and G" are constants for the materials I and II, respectively. This requires a minimum collector flux B_M in material I and A_M in material II. Thus, in the first stage, $A_1 = A_M + G''B$. The output A_M then enters the second stage as the control beam of transistor I (neglecting again the ac component). There it will produce amplified absorption $(-)G'A_M$ for the collector input beam B_2 so that the latter, by similar reason as before, should be $B_2 = B_M + G'A_M$.

Figure 9 shows the extension of this method to a transistor chain of n stages. Figure 9 displays the fact that, under the assumed special conditions, the input dc supply fluxes A and B remain the same for each stage except the first, where the input control beam is just the initial signal ΔA. However, although the dc input fluxes return periodically to the same values, ΔA continues to be amplified as it passes through the various stages. This is shown in Table 1 for the example of the input and output fluxes in transistor II of the second stage.

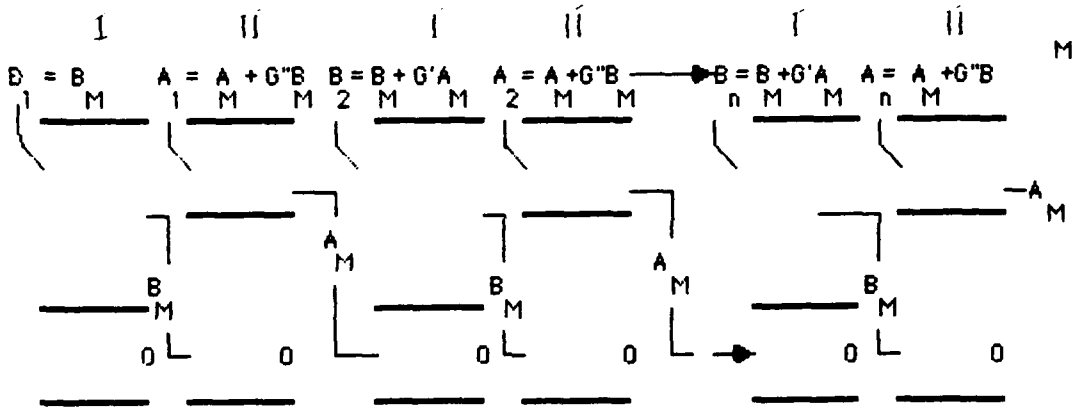

Figure 9. Example of dc flux flow in optical transistor chain.

Table 1

DC and AC Fluxes in Transistor II of Second Stage

Transistion	Input	Output
1-2	$B-G'A+G'G"B_M+(G')^2G"\Delta A$	0
2-3	$A_M+G"B-G'G"A+G'(G")^2B_M$	$A_M+(G'G")^2\Delta A$

In Table 1, the special relationships $A_1 = A_2 \ldots = A$, $B_1 = B_m$, and $B_2 \ldots = B$ have been used, where

$$A = A_M + G''B_M \tag{3-4}$$

$$B = B_M + G'A_M. \tag{3-5}$$

It will then be seen in Table 1 that when the control input is multiplied by $-G''$ and added to the input of the collector, the output of the collector is just $A_M + (G'G'')^2\Delta A$. By similar reasoning it is obvious that the n-stage signal photon gain equals

$$G_n = (G'G'')^n. \tag{3-6}$$

3.2.1 DC Flux Demands

As seen from Figure 9, the required supply of dc flux amounts to

$$P_{DC} = n(G'' + 1)B_M + n(G'+1)A_M - G'A_M. \tag{3-7}$$

The last term of Equation 3-7 results from the fact that the control input of the first transistor does not contain the dc component A_M, so that the term $G'A_M$ has to be deducted from the second term on the right.

A comparison of Equations 3-6 and 3-7 shows that the dc radiation demand increases linearly with the number n of stages, whereas the gain increases exponentially with n.

It will be understood that the condition of constant G' and G'', chosen for mathematical convenience, is unnecessary in practice. It is entirely possible to use flux quantities well below the quasi-asymptotic region (see Figure 8) so that the gains G' and G'' vary from a maximum, when the collector flux enters the transistor, to a minimum, when absorption has reduced the flux to A_M and B_M, respectively. The only difference is that in Equations 3-4 to 3-7, G'and G'' represent average

values which are somewhat complex to evaluate. Clearly, there will be values for A_M and B_M for which the efficiency of the dc fluxes is optimized.

Similarly, the complete absorption of the control beams represents only a special case. It is also possible to operate with the flux flow shown in Figure 7, although dc flux supply has to be added.

3.2.2 Signal-to-Noise Ratio (S/N)

For many applications of optical transistors, S/N values will be of critical importance. The noise in such transistors is photon noise arising mainly from two contributing sources: (1) fluctuations of the photon fluxes at the input of the first transistor, and (2) noise of the spontaneous emission which follows the absorption processes at the same frequency (although it is absent in radiationless transitions).

(1) We will at present assume (subject to a later further extension) that we are dealing with simple photon random noise as in (electronic) photomultipliers. Assume one observes an average number $\langle N \rangle$ of photons during an observation time Δt. Such observations will reveal fluctuations ΔN for which there exists the stochastic relationship

$$\langle (\Delta N)^2 \rangle = \langle N \rangle. \qquad (3\text{-}8)$$

Photon noise, which is the root-mean-square of deviations ΔN, therefore equals the square root of the average number of photons counted. The energy of a photon at 1 μm equals 2×10^{-19} Joule. At the first transistor an input collector flux B_M of 100 μW at 1 μm consists of 5×10^{14} photons per second, and these have a fluctuation of 2×10^{7} photons. Thus, during an observation time of one second, the noise of the dc input equals 4×10^{-12} Joule. A signal input of this energy yields then S/N = 1. More generally, the noise equivalent power (NEP) equals 4×10^{-12} watt-sec$^{1/2}$ under the assumed conditions which include a relatively small signal, hence a correspondingly small photon noise.

Just as for the dynode multiplication in electronic photomultipliers, succeeding stages do not add materially to the noise since the signal increases much faster than the dc supply.

(2) Even smaller is the noise contributed by fluctuations of spontaneous emission. Only a small fraction is within the acceptance angle of the beams. The accepted fluorescence noise is therefore small compared to that of the supply flux.

3.3 OPTICAL CONTINUUM TRANSISTORS

The transistor chain treated in the preceding sections consisted of discrete complementary transistor units. Among the possible alternatives of such chains, we selected the important extreme case in which the beam exciting the transition from level 1 to level 2 is completely absorbed in each pass through a transistor.

However, there exists another limiting case in which absorption is continuously compensated by dc supply (limit of thin complementary units). This extreme leads to a new type of transistor, with no electronic analog, in which materials I and II are homogeneously mixed. There results the "continuum transistor" shown schematically in Figure 10.

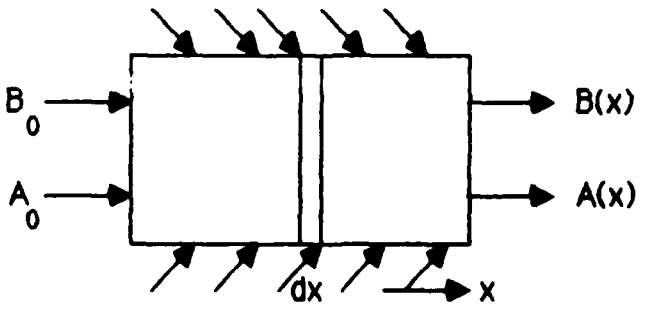

Figure 10. Scheme of continuum transistor.

Beams A_0 and B_0 are inputs to the device and pass through it in the x-direction. In addition, dc supply beams A_I and B_I enter the

material mixture, distributed over the length of the device. This "feed leakage" can be provided in various ways, such as evanescent waves or by other types of insertion. The excitation paths of beams A and B are those shown in Figure 7 (where, however, the dc supplies have been omitted). It is clear that beam A can only be absorbed by transitions between levels 1 and 2 in medium component I and, similarly, beam B only between levels 2 and 3 of component II of the mixture. Furthermore, the photon multiplication gains G'and G" remain the same as defined before.

We now assume that a concentration mixture of materials I and II is selected for a convenient absorption coefficient α. One obtains then for the incremental changes of A(x) and B(x) in an incremental interval dx as the balance of absorption and the constant feed supply A_I and B_I the following differential equations:

$$dA/dx = d(A - A_I)/dx = -\alpha(A - A_I) - \alpha G''(B - B_I) \tag{3-9}$$

$$dB/dx = d(B - B_I)/dx = -\alpha (B - B_I) - \alpha G'(A - A_I). \tag{3-10}$$

Multiplication of these equations by $\sqrt{G'}$ and $\sqrt{G''}$, respectively, yields the expressions

$$d[\sqrt{G'}\ (A - A_I)]/dx = -\alpha\sqrt{G'}\ (A - A_I) - \alpha\sqrt{G''}\ \sqrt{(G'G'')}\ (B - B_I) \tag{3-11}$$

$$d[\sqrt{G''}\ (B - B_I)]/dx = -\alpha\sqrt{G''}\ (B - B_I) - \alpha\sqrt{G'}\ \sqrt{(G'G'')}\ (A - A_I) \tag{3-12}$$

The solution of Equations 3-11 and 3-12 is given by

$$A(x) = A_I + (1/2)\ \{(A_0 - A_I) - (B_0 - B_I)\ \sqrt{(G''/G')}\}e^{-\alpha x[1 - \sqrt{(G'G'')}} \tag{3-13}$$

$$+ (1/2)\ \{(A_0 - A_I) - (B_0 - B_I)\ \sqrt{(G''/G')}\}e^{-\alpha x[1 + \sqrt{(G'G'')}}$$

$$B(x) = B_I - (1/2)\{(A_0 - A_I)\sqrt{(G''/G')} - (B_0 - B_I)\}e^{-\alpha x[1 - \sqrt{G'G''})]} \quad (3\text{-}14)$$

$$+ (1/2)\{(A_0 - A_I)\sqrt{(G''/G')} + (B_0 - B_I)\}e^{-\alpha x[1 + \sqrt{G'G''})]}$$

The gain of A(x) and B(x) with respect to the input A_0 is now, respectively,

$$dA(x)/dA_0 = (1/2)e^{-\alpha x[1 - \sqrt{(G'G'')}]} + (1/2)e^{-\alpha x[1 + \sqrt{(G'G'')}]} \quad (3\text{-}15)$$

$$dB(x)/dA_0 = -(1/2)\sqrt{(G''/G')}\{e^{-\alpha x[1 - \sqrt{(G'G'')}]} - e^{-\alpha x[1 + \sqrt{(G'G'')}]}\} \quad (3\text{-}16)$$

Equations 3-15 and 3-16 state that, for $\sqrt{(G'G'')} > 1$, the gain for A(x) is always larger than unity for a positive increment ΔA_0, while that for B(x) is negative (as is also the case for the basic complementary transistor unit). The inverse results for a positive ΔB_0 For practical purposes, the second term on the right of the two equations becomes negligible so that it is seen that the gain of A(x) grows exponentially as the beam passes along the x-direction.

3.3.1 DC Flux Demands in Continuum Transistor

The requirement for the dc photon supply to maintain the gains G'and G" is, as readily determined, per unit length of the medium:

$$P_A = \alpha A_I + \alpha G'' B_I \quad (3\text{-}17)$$

$$P_B = \alpha B_I + \alpha G' A_I \quad (3\text{-}18)$$

or

$$P_A + P_B = \alpha(G'+1)A_I + \alpha(G'' + 1)B_I. \quad (3\text{-}19)$$

Note that α is the reciprocal depletion length L'in the absence of gains G'and G". Because of the added absorption, the "effective" depletion length is by the factor (G'+1) or (G"+1) smaller. This is brought out by Equation 3-19. The total dc flux required for a continuum device of length L equals

$$P = L(P_A + P_B) \tag{3-20}$$

3.3.2 Comparison of Continuum and Discrete Unit Chains

It is of interest to compare the merits of the two limiting cases, although they differ apparently in specification, except for the molecular gains G'and G". The continuum device is characterized by a length L and absorption coefficient $\alpha = 1/L'$, whereas the discrete chain device is specified by the number n of complementary units. Nevertheless, a comparison is possible by interpreting a number n also for the continuum device.

3.3.2.1 DC Flux Demand

For the continuum device, one obtains with Equations 3-19 and 3-20 for the total dc demand, with $a = 1/L'$,

$$I = (L/L')(G' + 1)A_M + (L/L')(G" + 1)B_M \tag{3-21}$$

where, for purposes of comparison, we have replaced the index I by the index M.

The power required for the discrete unit chain is given by Equation 3-7, which contains the term $-G'A_M$ based on zero dc signal input of the first transistor, whereas an input A_0 (dc input A_M) was postulated for the continuum. One can do either for both devices, but for comparison we omit the term $-G'A_M$ in Equation 3-7 and obtain for the discrete unit chain of n stages

$$P = n(G' + 1)A_M + n(G'' + 1)B_M. \quad (3\text{-}22)$$

It is seen that Equation 3-21 for the continuum device is identical with Equation 3-22 if we define

$$n = L/L', \quad (3\text{-}23)$$

i.e., as the number of depletion lengths L' $(=1/\alpha)$ contained in the length L of the continuum transistor. This plausible result implies that the two transistor multiplier types require the same dc power.

3.3.2.2 Total Gain

Using Equation 3-23, we can now rewrite Equation 3-15 for $x = L$ of the continum device:

$$G_n = dA(L)/dA_0 = (1/2)e^{n(G_g - 1)} + (1/2)e^{-n(G_g + 1)} \quad (3\text{-}24)$$

where we have substituted the geometric mean G_g:

$$G_g = \sqrt{(G'G'')}. \quad (3\text{-}25)$$

For the discrete units device, we have from Equation 3-6 with Equation 3-25:

$$G_n = G_g^{2n} \quad (3\text{-}26)$$

We now compare the total gains obtained with Equation 3-24 for the continuum and with Equation 3-26 for the discrete units chain for $n = 10$. Table 2 presents this comparison for various values of the molecular mean gain G_g.

Table 2

Total Gain G_n for Continuum and Discrete Units Chains (n=10)

G_g	G_n - Discrete	G_n - Continuum
1.1	6.7	1.36
1.5	3.3×10^3	74
2.0	1.0×10^6	1.1×10^4
3.0	3.5×10^9	2.4×10^8
3.7	2.3×10^{11}	2.7×10^{11}
4.0	1.1×10^{12}	5.0×10^{12}

Table 2 demonstrates that for ten stages, the discrete units chain yields much higher photon multiplication than the continuum device for $G_g < 3.0$, but begins to fall behind the latter for $G_g > 3.7$. From the practical viewpoint, the continuum transistor has the often decisive advantage of monolithic structure. Thus, n = 30 stages with a $G_g = 1.5$ would pose considerable fabrication difficulties for the discrete complementary transistor chain, although it would yield a total gain of 3.7×10^{10}. However, continuum transistor construction with the same n and G_g would be a relatively easy task, yet have a still respectable gain of 1.6×10^6.

Finally, it is of interest to compare the results for setting, instead of Equation 3-23, $2n = L/L'$, for which the number depletion lengths in the continuum is twice the number of stages in the discrete chain. This also requires twice the dc supply power. However, for large n, the gain approaches the magnitude of that of the discrete chain since in the large-n limit, $e^{2n(G_g-1)} = G_g^{2n}$.

3.4 ADVANTAGES AND PROBLEMS FOR CASCADED OPTICAL TRANSISTORS

Optical complementary transistor systems, whether as continua or as chains of discrete units, were shown to offer very high photon multiplication factors even with rather low basic (or molecular) mean gain factors G_g, such as 1.5. It was also shown that, while the gain

increases exponentially with the number n of stages, the dc supply power grows only linearly with n. Finally, the signal-to-noise ratio is limited only by photon (shot) noise so that it can reach excellent values without the need for cooling.

However, it is important to stress that the rigid demands of complementary spectroscopic energy terms still pose a difficult task for identifying suitable combinations of materials. As described in Section 3.1.2, a search for such materials is underway, guided by the theoretical results described in this report. Perhaps the most important result is that mean basic gains of 1.5 or even lower suffice for very high total gains.

4. THE QUANTUM TRANSITION ETALON (QTE)

There exists, aside from the cascading of transistors, another method of achieving very high gain of the basic two-frequency interaction of beams in a simple three-level system. If the signal beam in its path through the medium is forced into many traversals by a Fabry-Perot etalon mirror configuration, relatively small control and signal powers can be expected to achieve high gain in "lossy etalon" operation. As pointed out before, the application of etalons for controlling the transmission of a beam at a single frequency is not a new concept. However, the combination of the two concepts, viz., (1) two-frequency quantum transition control and (2) multiple-pass interaction, results in more than just the possibility of enhancing conversion gain. The reason is that while transmittance and reflectance of an etalon are very sensitive to loss mechanisms within the cavity medium, the loss mechanisms themselves depend on the circulating power in the etalon via the stimulated emission process. This interaction in a device, called the *Quantum Transition Etalon (QTE),* results in a number of potentially useful effects.

Figure 11 shows schematically the beam configuration of the QTE. The active material, as before, represents essentially a three-level system in its interaction with two frequencies ν_{12} and ν_{23}. This material is contained between two mirrors that form the Fabry-Perot cavity. As shown in Figure 11, a control beam C with the frequency ν_{12} enters the etalon collinearly with a signal beam S_0 at frequency ν_{23}. The collinearity is not essential; in principle, beam C could pump the material inside the etalon at any angle. In contrast, beam S_0 enters the etalon at normal incidence, and the mirror spacing L of the etalon is adjusted for maximum transmission of the signal beam, i.e., $L = n\pi\lambda_{23}$ (n an integer).

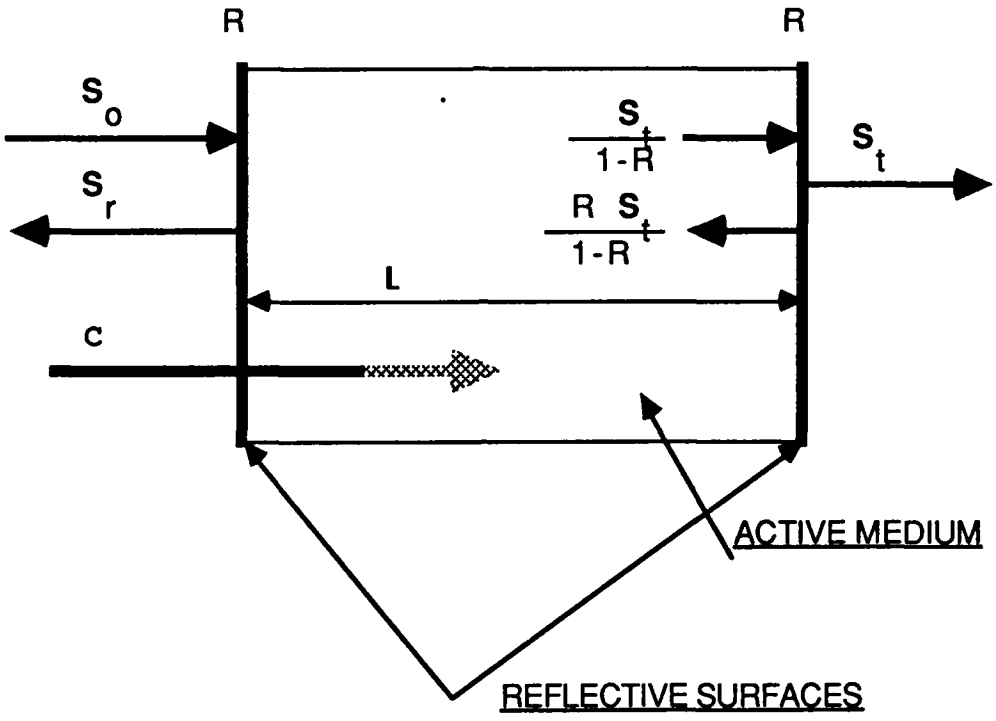

Figure 11. Fabry Perot quantum transition transistor (QTE).

In the absence of the control beam, the signal beam is transmitted essentially without attenuation through the device. When the control beam appears it generates a population in the intermediate level 2, thus causing an attenuation of the signal beam in a way similar to the one described before. However, because the interaction between the beams of signal and control takes place inside the etalon, where the signal field can be enhanced by resonance as much as several hundred times, the attenuation of the signal beam is much stronger than it would be in a single path device. In addition, as indicated before, the presence of stimulated emission introduces a more complex detailed behavior. In the following, an analysis is presented by which these detailed phenomena can be predicted.

4.1 THE LOSSY ETALON

We discuss first the etalon equations for an absorbing medium.

For an incident beam, S_o, we calculate the transmitted beam, S_t, and the reflected beam, S_r, as a function of the loss, L, in the etalon, where α is the induced loss coefficient per unit length in the active material. We define the single pass transmission in the etalon as

$$T = \exp(-\alpha L) \simeq 1 - \alpha L \tag{4-1}$$

where the approximation on the right is valid for small values of αL. Thus, in the absence of the etalon mirrors (i.e., R=0), $S_t = TS_o$, and the power, S_l, lost in the material by absorption equals $S_l = (1-T)S_o$. In the presence of etalon mirrors (R>0), however, the beam undergoes multiple absorption passes. Furthermore, since interference is possible only with wavetrains of decreasing amplitude, there will result a reflected beam of power, S_r.

Using reference 9 we find

$$S_t/S_0 = [T(1-R)^2]/[1-RT]^2 \tag{4-2}$$

and

$$S_r/S_o = [(1 - T)^2R]/[1 - RT]^2 \tag{4-3}$$

In the process of transmitting and reflecting these beams, the power lost inside the etalon is determined by

$$S_l = S_0 - (S_t + S_r) = [(1 + RT)(1+RT-T-R)]/[1-RT]^2S_0 \tag{4-4}$$

For the case of the conventional Fabry-Perot with no induced losses in the etalon, i.e., T=1, we see from these equations that

$$S_t = S_0$$
$$S_r = 0$$
$$S_l = 0$$

which means that the entire incident beam is transmitted, and there is no reflected beam or lost power in the etalon.

With a loss induced in the etalon, i.e., T≤1, the situation is different; the transmitted beam, S_t, is reduced by not only the amount of power absorbed in the etalon, S_l, but also by the generation of a reflected beam S_r. As an example we find that using R = 0.99 and changing the loss from 0.00 to 0.01, i.e., 1-T = 0.01, that

$$S_t = S_0 \rightarrow 0.25\ S_0$$
$$S_r = 0 \rightarrow 0.25\ S_0$$
$$S_l = 0 \rightarrow 0.50\ S_0$$

We see that the effect of introducing this relatively small loss is to decrease the signal beam 75% and to generate a reflected beam that is 25% of the incident beam.

The resonant signal power S_E inside the etalon, resulting from the beam multiplication, can be derived from the signal powers outside, and just inside, the output mirror, as shown in Figure 11. If the sum of the beam powers in the forward and backward direction has only a negligible variation across the length of the crystal, one obtains

$$S_E = [(1+R)/(1-R)]S_T \tag{4-5}$$

Expressing S_T in terms of the input power S_0 by Equation 4-2 yields

$$S_E = k\ S_0 = [T/(1-RT)^2]\ [(1-R)(1+R)]S_0 \tag{4-6}$$

which shows that the input power S_0 is enhanced inside the etalon by the factor

$$k = T(1-R^2)/(1-RT)^2 \tag{4-7}$$

Thus, for R = 0.990, the lossless etalon (T = 1.000) has an effective beam multiplication of k = 199. However, for R = 0.990 and T = 0.990,

Equation 4-7 yields for the multiplication k = 49.7. Thus, even a single-pass loss of only 1% reduces the multiplicator by a relatively large fraction which is the same as for the transmitted signal S_T for constant R, according to Equation 4-5.

Equation 4-5 has been derived using the linear approximation of Equation 4-1. For (1-T) = 0.01, the resulting error in Equation 4-7 for k can be ignored.

4.2 THE THREE-LEVEL PARTIALLY BLEACHED SYSTEM AS AN ETALON MEDIUM

The analysis in this section presents a synthesis (1) of the results obtained previously for the single-pass signal absorption in three-level materials, and (2) of the results for transmission and reflection in the lossy etalon. The procedure, in principle, is straightforward:

(1) Equations 2-22 to 2-25 in Section 2 are modified simply by replacing S with kS, where k is given by Equation 4-7. From this, one obtains the *single pass transmittance through the medium* $(S-S_0)/S_0 = 1-T = \alpha L$ as a function of k.

(2) Next, one introduces transmittance T into the etalon Equations 4-2 to 4-7 yielding equations for the transmitted beam S_t and the reflected beam S_r. However, because the etalon Equation 4-7 represents the multiplier as a function k = f(T), one obtains for S_t and S_r unwieldy cubic equations. Solutions, therefore, were obtained by computer. Alternatively, certain approximations led to solutions which clarified the physical processes involved and aided in the optimum choice of parameters.

The single-pass absorbance, 1-T, of the signal in the etalon is determined by the number densities N_2 and N_3 of the atomic states in levels 2 and 3, respectively. The population N_2 gives rise to Beer's Law type absorbing transitions (2→3), while N_3 increases transmission by stimulated emission (2←3) so that the net absorbance is given by

$$1-T = \alpha L = N_2\sigma_{32}[1 - (g_2/g_3)(N_3/N_2)]L;\ \alpha L << 1 \qquad (4\text{-}8)$$

where g_2 and g_3 are the respective statistical weights of the levels. The rate Equations 2-22 to 2-25 yield the expressions for N_2 and N_3 in the steady state which establishes itself after the relaxation times $1/\gamma_{12}$ and $1/\gamma_{23}$. Thus, N_2 results from the combination of the first three rate equations:

$$N_2 = P_c/[h\nu_{12}\gamma_{12}aL] \tag{4-9}$$

where P_c is the control power for the transition 1↔2. Equation 4-9 also follows, more directly, from the condition in this three-level system that the population in level 2 can only disappear in the balance by emission to level 1. Thus, P_c is the power required to replenish N_2 at the rate γ_{12} over the volume aL.

From Equation 2-23, one obtains directly N_3 in the convenient form

$$(g_2/g_3)(N_3/N_2) = (1 + S_h/kS_0)^{-1} \tag{4-10}$$

where

$$S_h = (g_3/g_2)(\gamma_{23}/\sigma_{32})ah\nu_{23} \tag{4-11}$$

as defined in Section 2, Equation 2-27. Note that S_h/kS_0 in Equation 4-10 is proportional to the ratio of the spontaneous emission rate to the rate of emission stimulated by kS_0. As this ratio is varied from large to small values, the level 3 population changes from relatively small values to saturation as should be expected.

Introduction of Equation 4-10 into Equation 4-8, yields now an implicit expression for the single-pass absorption:

$$1-T = \sigma_{32}N_2[1 - (1 + S_h/kS_0)^{-1}]L = \sigma_{32}N_2[S_h/(S_h+kS_0)]L \tag{4-12}$$

It is of interest for the alternative modes of QTE operation that the denominator in Equation 4-12 contributes separately to the two ways in

which the population in level 3 can return to level 2. According to Equation 4-11, S_h is proportional to the spontaneous emission (fluorescence) rate γ_{23}, whereas kS_0 is the term proportional to the rate of stimulated emission. Thus, for $S_h >> kS_0$, Equation 4-12 reverts to Beer's law, whereas for $S_h << kS_0$, Equation 4-12 reverts to the limit of transparency. We shall refer to the ratio S_h/kS_0 as the *fluorescence parameter*.

If in Equation 4-12 N_2 is now substituted by Equation 4-9, one obtains for the single-pass absorption in the etalon medium

$$1-T = G_{sat}P_c(S_h + kS_0)^{-1} \qquad (4\text{-}13)$$

where $G_{sat} = (\upsilon_{23}/\upsilon_{12})(\gamma_{23}/\gamma_{12})(g_3/g_2)$ represents the saturation gain (i.e., the asymptotic limit of gain for k=1) of single-pass absorption introduced in Equation 2-27. According to Equation 4-7, the beam multiplier k equals $T(1-R^2)/(1-RT)^2$. Thus, Equation 4-13 is a cubic equation in T as a function of an operational variable, such as $T = T(P_c)$ or $T(S_0)$. Corresponding cubic equations are obtained for the signals transmitted and reflected by the etalon, viz., S_t and S_r, according to Equations 4-2 and 4-3, respectively. Cubic equations have three solutions, or roots, and each set of roots corresponds to a branch of the resulting functions, such as $T(P_c)$. However, two roots, or all three, may be equal. Furthermore, certain roots may be complex or, if real, may not be allowed by the conditions of operation. An example is the solution of the quadratic equation for the transmittance $T(S_t)$ from Equation 4-2 which results in two values of T for any S_t. Here one of the roots, for which $T>1/R$, is not allowed by the postulated physical conditions since it amounts to $T>1$ *(negative absorption)* which is valid for a lasing medium.

4.2.1 Parameters and Examples

To put the results obtained, explicitly or implicitly, in the derived analytical expressions into perspective, we proceed in the

following with the choice of examples for the parameters of the device and for the variables of its operation. Table 3 presents such choices and their effect on the device performance for lithium as medium. For greater depth, the range of certain variables, notably of the single-pass absorption, 1-T, has been extended in Table 4.

The device is a Fabry-Perot etalon containing, between its mirrors, an active medium (the three-quantum level material). The construction parameters of the device are, first, the spectroscopic data of the medium which are fixed by the choice of the material. For simplicity (because the data are available from tables and our own evaluations), we choose lithium as the medium. A second parameter is the mirror reflectivity for which we have selected two values, viz., 0.990 and 0.999, as shown in Column C of Table 3. The third etalon parameter, viz., the mirror spacing L, cancels out in our equations for the order of approximation used for them. Furthermore, the cross-sectional area of the etalon enters only as a proportionality factor for the applied radiation powers. Tables 3 and 4 have been computed for fiber dimensions of 40 μm diameter.

There exist for this device also two variables of operation: (1) the signal input power, S_o, listed in Column A, for several values differing in Table 3 by steps of the factor 4; and (2) the control power P_c assumed to be totally absorbed and listed in Column D.

The choice of instrument parameters and operational variables now determines all propagation characteristics of control and signal as shown in the rest of the tables. However, because these propagation characteristics appear as exceedingly complex cubic roots of expressions containing the parameters and operational variables, a much simpler "parametric" approach was followed (see Table 3). First the single-pass absorption, 1-T, was chosen (Column B) so that the beam multiplication factor k (Column E) could be obtained with Equation 4-7. P_c (Column D) then follows from Equation 4-13 with T and k. The transmitted signal S_t (Column F) and the reflected signal S_r (Column H) are obtained from

Table 3

QTE Etalon Performance for Lithium

	A	B	C	D	E	F	G	H	I	J
1	SIGNAL-	SINGLE PASS	MIRROR	CONTROL	BEAM	TRANSM.	DIFFERENTIAL	REFLECTED	DIFFERENTIAL	ABS IN
2	INPUT	ABSORPTION	REFLECTION	POWER	MULT.	SIGNAL	GAIN	SIGNAL	GAIN	ETALON
3	So (μW)	1-T	R	Pc (μW)	k	St(μW)	∂St/∂Pc	Sr (μW)	∂Sr/∂Pc	Sia(μW)
4	0.50	0.00	0.990	0.00	199.00	0.50	-5.7	0.00	0.0	0.00
5	0.50	0.01	0.990	0.11	49.75	0.12	-1.4	0.12	1.4	0.25
6	2.00	0.01	0.990	0.18	49.75	0.50	-5.5	0.50	5.5	1.00
7	8.00	0.01	0.990	0.43	49.75	2.00	-22.2	2.00	22.2	4.00
8	32.00	0.01	0.990	1.43	49.75	8.00	-93.9	8.00	93.9	16.00
9	128.00	0.01	0.990	5.44	49.75	32.00	-493.7	32.00	493.7	64.00
10	256.00	0.01	0.990	10.79	49.75	64.00	-1,699.6	64.00	1,699.6	128.00
11	0.50	0.02	0.990	0.20	21.96	0.06	-0.4	0.22	0.8	0.22
12	2.00	0.02	0.990	0.26	21.96	0.22	-1.9	0.89	3.8	0.89
13	8.00	0.02	0.990	0.48	21.96	0.88	-14.6	3.57	29.3	3.55
14	32.00	0.02	0.990	1.37	21.96	3.53	20.9	14.27	-42.1	14.20
15	128.00	0.02	0.990	4.91	21.96	14.13	13.0	57.08	-26.1	56.80
16	256.00	0.02	0.990	9.63	21.96	28.25	12.2	114.16	-24.6	113.59
17	0.50	0.04	0.990	0.38	7.77	0.02	-0.1	0.32	0.4	0.16
18	2.00	0.04	0.990	0.42	7.77	0.08	-0.4	1.29	1.5	0.63
19	8.00	0.04	0.990	0.58	7.77	0.31	-2.2	5.15	8.8	2.54
20	32.00	0.04	0.990	1.21	7.77	1.25	12.5	20.60	-50.8	10.15
21	128.00	0.04	0.990	3.71	7.77	4.99	4.6	82.41	-18.8	40.59
22	256.00	0.04	0.990	7.05	7.77	9.99	4.2	164.83	-17.1	81.18
23	0.50	0.08	0.990	0.75	2.30	0.01	0.0	0.40	0.1	0.10
24	2.00	0.08	0.990	0.77	2.30	0.02	-0.1	1.59	0.5	0.38
25	8.00	0.08	0.990	0.86	2.30	0.09	-0.3	6.37	2.3	1.54
26	32.00	0.08	0.990	1.23	2.30	0.37	-2.2	25.48	18.3	6.15
27	128.00	0.08	0.990	2.72	2.30	1.48	2.8	101.93	-23.6	24.59
28	256.00	0.08	0.990	4.70	2.30	2.96	2.1	203.86	-17.1	49.18
29	0.50	0.01	0.999	0.10	16.39	0.00	-0.1	0.41	0.9	0.08
30	2.00	0.01	0.999	0.12	16.39	0.02	-0.4	1.65	4.3	0.33
31	8.00	0.01	0.999	0.20	16.39	0.07	-97.9	6.62	983.0	1.32
32	32.00	0.01	0.999	0.53	16.39	0.26	1.8	26.47	-17.7	5.27
33	128.00	0.01	0.999	1.85	16.39	1.05	1.4	105.87	-14.1	21.08
34	256.00	0.01	0.999	3.62	16.39	2.10	1.4	211.74	-13.6	42.16
35	0.50	0.02	0.999	0.19	4.45	0.00	0.0	0.45	0.2	0.04
36	2.00	0.02	0.999	0.20	4.45	0.00	-0.1	1.82	1.0	0.18
37	8.00	0.02	0.999	0.24	4.45	0.02	-0.3	7.26	5.3	0.72
38	32.00	0.02	0.999	0.42	4.45	0.07	3.8	29.05	-75.8	2.88
39	128.00	0.02	0.999	1.14	4.45	0.28	0.8	116.20	-15.8	11.51
40	256.00	0.02	0.999	2.10	4.45	0.57	0.7	232.41	-14.0	23.02
41	0.50	0.04	0.999	0.37	1.14	0.00	0.0	0.48	0.1	0.02
42	2.00	0.04	0.999	0.38	1.14	0.00	0.0	1.91	0.3	0.09
43	8.00	0.04	0.999	0.40	1.14	0.00	0.0	7.62	1.1	0.37
44	32.00	0.04	0.999	0.49	1.14	0.02	-0.1	30.49	6.0	1.49
45	128.00	0.04	0.999	0.86	1.14	0.07	1.2	121.95	-50.1	5.98
46	256.00	0.04	0.999	1.35	1.14	0.15	0.5	243.90	-19.6	11.96
47	0.50	0.08	0.999	0.74	0.28	0.00	0.0	0.49	0.0	0.01
48	2.00	0.08	0.999	0.74	0.28	0.00	0.0	1.95	0.1	0.05
49	8.00	0.08	0.999	0.75	0.28	0.00	0.0	7.81	0.3	0.19
50	32.00	0.08	0.999	0.80	0.28	0.00	0.0	31.25	1.1	0.75
51	128.00	0.08	0.999	0.98	0.28	0.02	-0.1	124.98	6.4	3.00
52	256.00	0.08	0.999	1.22	0.28	0.04	-0.3	249.96	27.3	6.00

Table 4

Details of Values Near Apex for Lithium at S_o=125 μW

	A	B	C	D	E	F	G	H	I	J
1	SIGNAL-	SINGLE PASS	MIRROR	CONTROL	BEAM	TRANSM.	DIFFERENTIAL	REFLECTED	DIFFERENTIAL	ABS IN
2	INPUT	ABSORPTION	REFLECT.	POWER	MULT.	SIGNAL	GAIN	SIGNAL	GAIN	ETALON
3	So (μW)	1-T	R	Pc (μW)	k	St(μW)	∂St/∂Pc	Sr (μW)	∂Sr/∂Pc	Sia(μW)
4	125.00	0.008	0.99	5.194	65.05	40.86	-54.2	22.93	43.2	61.21
5	125.00	0.008	0.99	5.199	64.68	40.63	-55.4	23.10	44.5	61.27
6	125.00	0.008	0.99	5.204	64.31	40.40	-56.7	23.28	45.8	61.33
7	125.00	0.008	0.99	5.209	63.94	40.17	-58.0	23.45	47.2	61.38
8	125.00	0.008	0.99	5.214	63.58	39.94	-59.4	23.62	48.6	61.44
9	125.00	0.008	0.99	5.219	63.22	39.71	-60.9	23.80	50.1	61.49
10	125.00	0.008	0.99	5.223	62.87	39.49	-62.5	23.97	51.7	61.54
11	125.00	0.008	0.99	5.227	62.51	39.27	-64.1	24.15	53.4	61.59
12	125.00	0.008	0.99	5.232	62.16	39.05	-65.8	24.32	55.1	61.63
13	125.00	0.008	0.99	5.236	61.82	38.83	-67.6	24.49	57.0	61.68
14	125.00	0.008	0.99	5.240	61.47	38.61	-69.5	24.66	59.0	61.72
15	125.00	0.008	0.99	5.244	61.13	38.40	-71.6	24.84	61.0	61.77
16	125.00	0.008	0.99	5.247	60.79	38.19	-73.7	25.01	63.2	61.81
17	125.00	0.008	0.99	5.251	60.46	37.98	-76.0	25.18	65.6	61.85
18	125.00	0.008	0.99	5.255	60.13	37.77	-78.4	25.35	68.1	61.88
19	125.00	0.008	0.99	5.258	59.80	37.56	-81.0	25.52	70.7	61.92
20	125.00	0.008	0.99	5.261	59.47	37.35	-83.8	25.69	73.5	61.96
21	125.00	0.008	0.99	5.265	59.14	37.15	-86.7	25.86	76.6	61.99
22	125.00	0.008	0.99	5.268	58.82	36.95	-89.9	26.03	79.8	62.02
23	125.00	0.008	0.99	5.271	58.50	36.75	-93.3	26.20	83.3	62.06
24	125.00	0.009	0.99	5.274	58.18	36.55	-97.0	26.37	87.1	62.09
25	125.00	0.009	0.99	5.276	57.87	36.35	-100.9	26.53	91.2	62.12
26	125.00	0.009	0.99	5.279	57.56	36.15	-105.3	26.70	95.6	62.14
27	125.00	0.009	0.99	5.282	57.25	35.96	-110.0	26.87	100.4	62.17
28	125.00	0.009	0.99	5.284	56.94	35.77	-115.1	27.04	105.7	62.20
29	125.00	0.009	0.99	5.286	56.64	35.58	-120.7	27.20	111.5	62.22
30	125.00	0.009	0.99	5.289	56.33	35.39	-127.0	27.37	117.9	62.24
31	125.00	0.009	0.99	5.291	56.03	35.20	-133.9	27.54	124.9	62.27
32	125.00	0.009	0.99	5.293	55.74	35.01	-141.6	27.70	132.8	62.29
33	125.00	0.009	0.99	5.295	55.44	34.83	-150.2	27.87	141.7	62.31
34	125.00	0.009	0.99	5.297	55.15	34.64	-159.9	28.03	151.7	62.33
35	125.00	0.009	0.99	5.299	54.86	34.46	-171.0	28.20	163.1	62.34
36	125.00	0.009	0.99	5.300	54.57	34.28	-183.8	28.36	176.1	62.36
37	125.00	0.009	0.99	5.302	54.29	34.10	-198.6	28.52	191.3	62.38
38	125.00	0.009	0.99	5.304	54.00	33.92	-215.9	28.69	209.1	62.39
39	125.00	0.009	0.99	5.305	53.72	33.74	-236.6	28.85	230.4	62.41
40	125.00	0.009	0.99	5.307	53.44	33.57	-261.7	29.01	256.1	62.42
41	125.00	0.009	0.99	5.308	53.16	33.39	-292.8	29.18	288.0	62.43
42	125.00	0.009	0.99	5.309	52.89	33.22	-332.2	29.34	328.4	62.44
43	125.00	0.009	0.99	5.310	52.62	33.05	-383.8	29.50	381.3	62.45
44	125.00	0.010	0.99	5.311	52.35	32.88	-454.3	29.66	453.7	62.46
45	125.00	0.010	0.99	5.312	52.08	32.71	-556.7	29.82	558.8	62.47
46	125.00	0.010	0.99	5.313	51.81	32.54	-718.5	29.98	724.8	62.48
47	125.00	0.010	0.99	5.314	51.55	32.38	-1,013.0	30.14	1,026.9	62.48
48	125.00	0.010	0.99	5.315	51.28	32.21	-1,716.0	30.30	1,748.2	62.49
49	125.00	0.010	0.99	5.316	51.02	32.05	-5,604.5	30.46	5,738.2	62.49
50	125.00	0.010	0.99	5.316	50.76	31.89	4,428.4	30.62	-4,556.2	62.50
51	125.00	0.010	0.99	5.317	50.51	31.73	1,587.4	30.78	-1,641.2	62.50

Equations 4-2 and 4-3, respectively. Finally, the differential gains (slopes) dS_t/dP_c and dS_r/dP_c (Columns G and I, respectively) are determined by using very small steps in ΔP_c by the computer.

The first data point in Table 3 (Row 4) is the condition of $P_c=0$ (zero control power), for which there is no absorption of the signal beam, so that the device operates like the ideal conventional Fabry-Perot etalon. Also at this point, the signal power circulating within the etalon has the maximum value it can have, viz., about $2S_o/(1-R)$. Upon application of the control power, the signal power is more or less drastically absorbed, resulting in a corresponding reduction of k. In turn, this results in the appearance of a reflected signal. Thus, as discussed before, with R=0.99 and (1-T)=0.01, i.e., for 1% single pass absorption, there result transmitted and reflected signals, each equal to 0.25 S_o, i.e., one quarter of the input signal power. This example is evaluated for six S_o-values in Rows 5-10 of Table 3. For example, S_o = 32 μW yields 8 μW for the transmitted and reflected beams each and requires 1.43 μW of control power P_c. The net absorption is 50%, which reduces the internal power multiplication factor to 49.75.

The gains in transmission and reflection in this case are, respectively, -94 and +94. The positive gain in reflection may be particularly important since it occurs at P_c=1.43 μW against a background of S_r=0 at P_c=0.

Tables 3 and 4 present a survey of the effects caused by stepwise varying the essential parameters of operation and instrumentation. Inspection of the tables reveals a considerable number of performance features which have to be explored in greater detail. Perhaps the most important of these is the reversal of sign in the slopes of S_t and S_r (Columns G and I) which occurs for larger signal input powers. In a purely mathematical evaluation, disregarding limits imposed by the physical situation, up to three branches for $S_t(P_c)$ and $S_r(P_c)$ can be expected. Where it is physically admissable, however, double- or triple-valued functions imply the possibility of bistability, especially for large values of the signal power.

No bistability is expected if the signal beam encounters only absorption by the population N_2, but encounters no stimulated emission from the level N_3, that is, if $N_3/N_2 << 1$. The reason is that this condition corresponds to the "Beer's law limit" $S_h >> kS_o$ in Equation 4-12, which is far below the bleaching limit of the level 2↔3 transition.

Figures 12 and 13 represent a computer-generated comparison of the transmission and reflection behavior when stimulated emission is absent or, respectively, present in this model. For both cases, instrumental parameters and operating conditions are assumed to be the same (excepting the different scales for P_c), viz., S_h = 110 μW (lithium where also G_{sat} = 11.9), S_o = 128 μW, and R = 0.990. Figure 12 shows that in the absence of stimulated emission (a purely <u>hypothetical</u> case for the assumed magnitudes), the transmitted signal power very rapidly decreases from the 128 μW input, as P_c increases from zero, and then approaches zero asymptotically. Meanwhile the reflected power rises more gradually to a value approaching the signal input power. Thus, the operation of the etalon proceeds for increasing P_c from total transmission to almost total reflection.

However, under the conditions selected in this example, it is clearly seen on the basis of Tables 3 and 4 that the condition $S_h >> kS_o$ is in <u>reality</u> far from being fulfilled, at least for the qualifying set of points in which S_o = 128 μW and k>1. For an absorption, e.g., of 1% (1-T = 0.01), kS_o equals more than 6000, far larger than S_h. In fact, the curves of Figure 13 are more less dominated by the stimulated emission process, as will be explained in chapter 5.

A comparison of Figures 12 and 13 reveals that the existence of stimulated emission causes, at least in the mathematical model, two branches of operation each for transmitted and reflected power as functions of the control power.

The upper branch of the transmission curve proceeds with increasing downward slope as P_c is increased from zero until, at P_c = 5.35 μm, it reaches the maximum of required control power (cf. Row

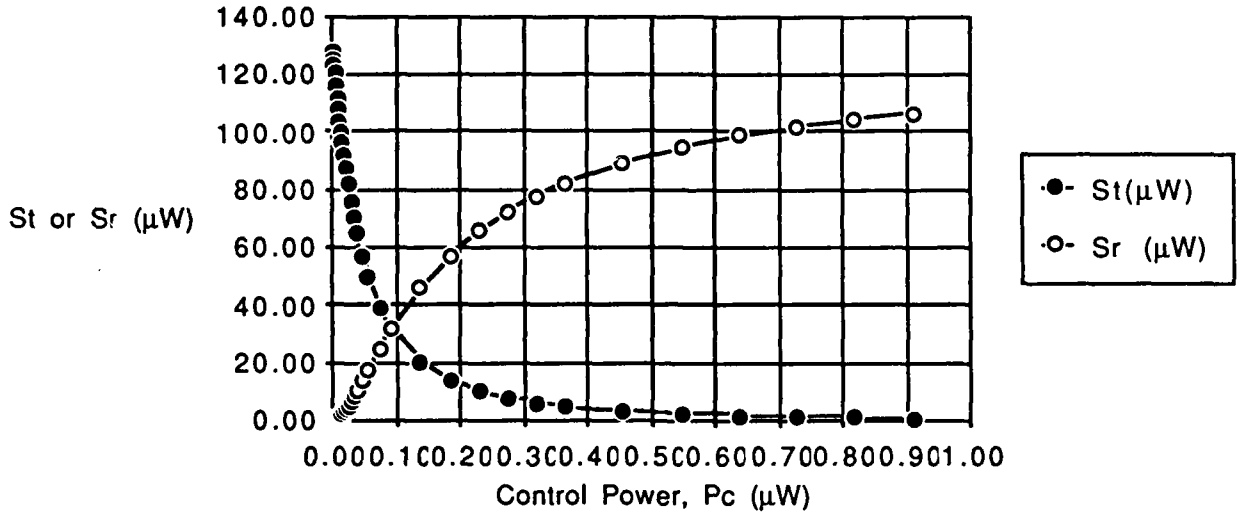

Figure 12. Transmitted and reflected power in QTE in the absence of stimulated emission.

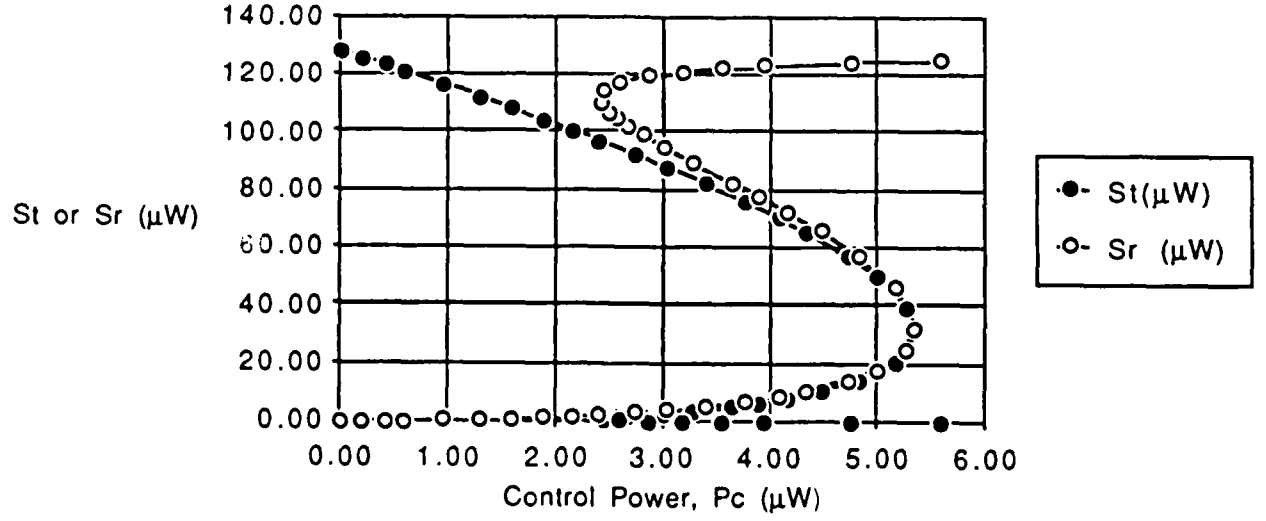

Figure 13. Transmitted and reflected power in QTE in the presence of stimulated emission.

10 of Table 3). At this point it meets the corresponding branch of the reflection curve which has increased to this point from zero. This point, then, is the starting point for the second branches, viz., downward with decreasing P_c for transmitted power, upward for reflected power. It is likely that this behavior leads to a bistable operation between the two pairs of branches.

Figure 14 shows graphically a comparison between a lossless etalon and QTE etalon operating with S_o = 128 μW and P_c = 2.7 μW. The large reflected power (102 μW) and small transmitted power show that this working point belongs to the second pair of operating branches. The demonstration of a device with such operating characteristics can form the bases for very powerful optical devices, among them high-gain optical amplifiers.

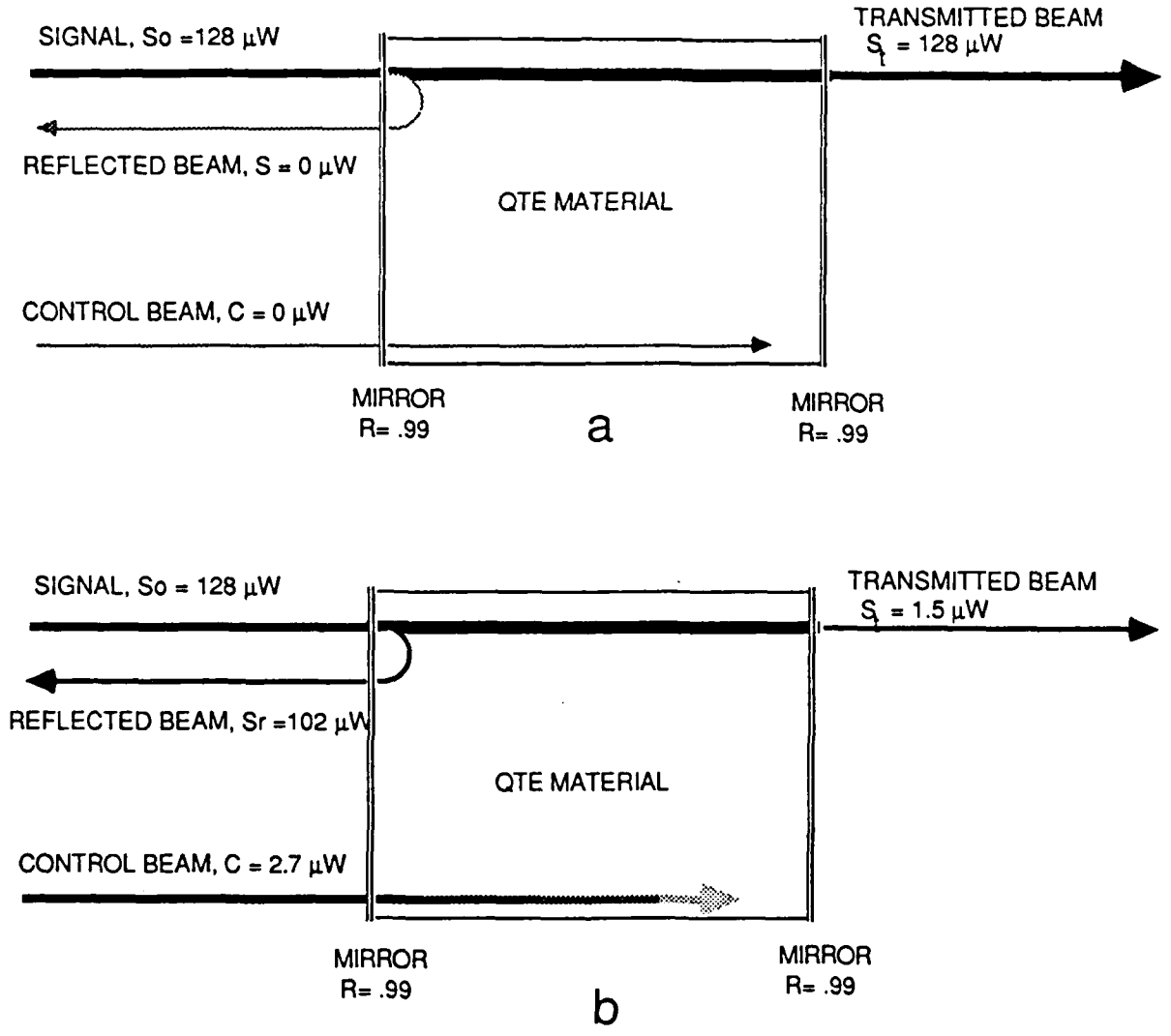

Figure 14. Transmitted and reflected beams in lithium QTD.

5. QTE: ALTERNATIVES OF OPERATION

The preceding three sections have introduced and analyzed three concepts for optical transistor and switches: (1) A basic three-level system; (2) an amplifier device which uses two complementary three-level materials either in cascade or as a monolithic mixture; and (3) the quantum transition etalon (QTE) which uses the basic three-level system as active material inside an etalon. Practical considerations argue for selecting the QTE as the most promising solution and, therefore, for further exploration. In transistor operation, the basic system (1) has a gain, dS_t/dP_c, limited to about 12. The amplifier system (2) has, in principle, unlimited gain, but it requires the matching of two three-level materials with a double coincidence in which transitions υ_{12} of the first material must overlap υ_{23} of the second and, likewise, υ_{23} of the first material with υ_{12} of the second. The QTE (3) has the simplicity of the first concept and promises the high gain of the second concept. One of the distinguishing features of the QTE transistor is the gain of either the transmitted or the reflected beam power at one frequency with respect to the beam power at another frequency. It remains to be shown that high gains can actually be achieved in stable operation.

5.1 ANALYSIS OF GAIN BEHAVIOR

Although the computer program readily yields dS_t/dP_c and dS_r/dP_c for any combinations of parameters and operating conditions, the optimum choice of such combinations is best guided by theory. The physical phenomena giving rise to the results obtained can, in fact, be understood only with the analysis.

The gains dS_t/dP_c and dS_r/dP_c can be derived with the previously introduced relations (see Equations 4-2, 4-3, 4-13, and 4-7, respectively) as follows:

$$S_t = [T(1-R^2)/(1-TR)^2]S_0 \quad (5\text{-}1)$$

$$S_r = [R(1-T^2)/(1-TR)^2]S_0 \quad (5\text{-}2)$$

$$1-T = G_{sat}P_c(S_h+kS_0)^{-1} \quad (5\text{-}3)$$

with

$$k = T(1-R^2)/(1-TR)^2 \quad (5\text{-}4)$$

For the gain in transmission, one can write

$$dS_t/dP_c = (dS_t/dT)(dT/dP_c) \quad (5\text{-}5)$$

With Equations 5-1 to 5-5, there results, after the appropriate and somewhat lengthy substitutions, for the transmission gain:

$$dS_t/dP_c = G_{sat}(1-R)(1+TR)/\{(1+R)[(1-2T+TR)-T(1-TR)S_h/kS_0]\} \quad (5\text{-}6)$$

By an analogous procedure, one obtains for the gain in reflection:

$$dS_r/dP_c = -2G_{sat}R(1-T)/\{(1+R)[(1-2T+TR) - T(1-TR)S_h/kS_0]\} \quad (5\text{-}7)$$

Comparison of Equations 5-6 and 5-7 shows that the gains for transmission and reflection have opposite signs, a result of the fact that an etalon at resonance has increasing reflection as transmission decreases. Aside from that, the two equations show a difference only in the nominator. For R=0, the situation reverts to the basic single-pass optical transistor discussed in Section 3. In this case, $dS_r/dP_c = 0$ and $dS_t/dP_c = -G_{sat}(1 + S_h/S_0)^{-1}$ with the approximation used in the QTE analysis, viz., $(1-T) << 1$.

The sign of the gains or slopes given by Equations 5-6 and 5-7 are of particular interest and can be correlated to the various interacting physical phenomena at play. It will be seen that, in the nominators, the signs remain the same for any admissable values of T or R. The denominator, however, can change sign, as can be seen by isolating S_h/kS_0 from the ratio Q defined by

$$Q \equiv (1-2T+TR)/T(1-TR) \tag{5-8}$$

The sign of the denominator of the gain equations is determined by the difference D:

$$D = Q - S_h/kS_0 \tag{5-9}$$

This equation compares the fluorescence parameter, which indicates the ratio of signal absorption after k passes to stimulated emission, with a parameter Q, which reflects the etalon action on signal transmission and reflection (notwithstanding the fact that k is a function of R and T).

Class I Operation. A special case (Class I) is the condition

$$S_h/kS_0 >> |Q| \tag{5-10}$$

For this limit, which can be maintained for the entire operating range of the control power P_c, the denominator remains negative.
Equation 5-10 corresponds to the condition that signals of very small incident power S_0 encounter in level 2 a population which is much larger than that which they can generate in level 3. Absorption, in this limit, follows Beer's law and proceeds without stimulated emission for the 2→3 transition. The powers of transmitted beams, S_t, then decrease, and of reflected beams, S_r, increase, as monotonic functions of increasing P_c.

Class II Operation. For smaller values of the fluorescence parameter S_h/k_S (Class II) stimulated emission becomes important giving rise to multiple branches of $S_t(P_c)$ and $S_r(P_c)$, as briefly described in the following. According to Equations 5-6 and 5-7, the respective starting slopes, at P_c=0 and T=1, are $dS_t/dP_c = -G_{sat}/(1+S_h/kS_0)$ and $dS_r/dP_c = 0$. At this point, the etalon medium is closest to saturation. However, as P_c and, subsequently, the single-pass absorption, 1-T, begin to increase, the function Q(T) proceeds from negative toward positive values. The turning point, Q=0, is reached for a value T_t which is approximately equal to R, but is more exactly given by

$$T_t = (2\text{-}R)^{-1}, \qquad 1\text{-}T_t = (1\text{-}R)/(2\text{-}R) \qquad \text{for } Q = 0 \qquad (5\text{-}11)$$

The increase of (1-T) thus first reduces the denominator in the slope equations and increases the absolute amounts of the gains. This corresponds to the lossy etalon behavior of increasing signal reflection at the expense of transmission. When Q has become positive, there is a point at which $Q = S_h/kS_0$ so that the denominator of the slope equations vanishes and the gains are infinite. There results the apex and a second branch in which the denominator of the gain curves is positive. Meanwhile, according to Equation 4-4, k decreases monotonically, as (1-T) increases. Thus, the fluorescence parameter, as k collapses, increases faster than Q, so that the denominator of the slopes vanishes again and a third branch results. Ultimately, k is small enough so that condition 5-10 is valid.

The three branches expected for the general case on the basis of this analysis represent the three solutions of cubic equations of the form $S_t^3 + pS_t^2 + qS_t + r = 0$. The three branches are shown in Figure 13. The calculations for the third branch, however, have only the merit of indicating the trend of the branch since the condition $(1\text{-}T) \ll 1$ used in Equation 5-8 is not fulfilled.

The calculation of optimized parameters and the insight into the interaction of stimulated emission, absorption, and multiple beam interference can be substantially simplified. We introduce the symbols $\rho = (1\text{-}R)$ and $\tau = (1\text{-}T)$ into Equations 5-6 and 5-7 and assume that

$$\rho \ll 1 \text{ and } \tau \ll 1 \qquad (5\text{-}12)$$

In first order, then, R = 1 and T = 1, $(1\text{-}TR) = -(\tau+\rho)$, and $\tau\rho \ll (\tau+\rho)$. This shortens Equations 5-6 and 5-7 to

$$dS_t/dP_c \simeq G_{sat}\rho/[(\tau - \rho) - 1/2(\tau + \rho)^3 S_h/\rho S_0] \qquad (5\text{-}13)$$

$$dS_r/dP_c \simeq -G_{sat}\tau/[(\tau - \rho) - 1/2(\tau + \rho)^3 S_h/\rho S_0)] \qquad (5\text{-}14)$$

The two equations differ only in the nominators $G_{sat}\rho$ and $-G_{sat}\tau$, respectively, viz., the nominator for the transmitted beam is proportional to the mirror transmittance ρ, that for the reflected beam is proportional to the single-pass absorption τ.

Second order corrections of Equations 5-13 and 5-14 involve such terms as $(\tau+\rho)^2$. This consideration is important for evaluating the conditions under which the denominator in square brackets of these equations vanishes and the gains become very high. For example, if $\tau \simeq 0.02$ and $\rho \simeq 0.01$, the exact values of these variables for the zero point of the denominator are determined by the two equations with 3% accuracy. However, if the difference value within the square brackets becomes of the order of this error, the absolute values of the gains in this region can only be determined if the two equations are extended to higher orders.

5.2 DYNAMIC EFFECTS AND BISTABILITY

The analysis in Section 5.1 has shown that the characteristics of QTE operation fall into two classes.

In Class I, fluorescence is dominant over stimulated emission in the 3→2 transition for the entire range of the control power P_c. Class I has ony a single branch of operation. The denominator of Equations 5-13 and 5-14 remains negative because the magnitude of the negative second term has no upper limit, whereas the first term cannot have a positive value larger than unity. Class I operation is, therefore, always stable. Fluctuations of beam power have no effect on this stability except for the important case in which the choice of the variables borders Class II operation over a certain region yielding high gains.

Class II represents the more general case in which either fluorescence or stimulated emission may be dominant depending on the choice of control power P_c or on a memory effect of operation. As has been described in Section 5.1, there result, *as mathematical solutions,* three branches of values for QTE signal beam transmission and

reflection. The *physical existence* of these three branches, however, has now to be examined.

Operation in the branch with the highest transmission (lowest reflection) is initiated when, with the incident signal S_0 already present, the control power P_c is introduced at a level below that producing the apex. At P_c near zero, the transition 2→3 is nearly bleached and the single-pass absorption τ is near zero. The dominance of stimulated emission remains intact, as stable operation, until P_c reaches the value it has at the apex.

In contrast, if a sufficient amount of control power P_c is first applied, the subsequently introduced signal S_0 encounters a relatively large population in level 2 and almost none in level 3. Starting under a condition of relatively large single-pass absorption, hence small beam multiplication, k, the signal is dominated by the fluorescence parameter, S_h/kS_0, and this to an increasing degree as P_c increases. Thus, the third branch of lowest transmission and highest reflection results as a stable operation.

When experimental conditions proceed on the first branch, with P_c increasing beyond the apex value, the positive (negative) slope for transmission (reflection), which is the characteristic for the second branch, does not materialize. This latter process would result in a reduced demand on control power, whereas, in fact, P_c is increased, the same fraction being absorbed in the transition 1→2. The excess power thus produces discontinuously the conditions for the third branch, bypassing the second branch. A similar argument applies to operation on the third branch, with P_c decreasing from high values to the value at the second apex. Again, the turn into the second branch is bypassed by a discontinuous transition, and in this case, to the first branch.

The behavior of the QTE in Class II operation is summerized in Figure 15. As indicated by the arrows, it has been assumed that the control power P_c is applied after a fixed incident signal S_0 has been introduced first, P_c varying from zero to a value well above the first apex and back to zero. Thus, Class II operation is bistable, limited

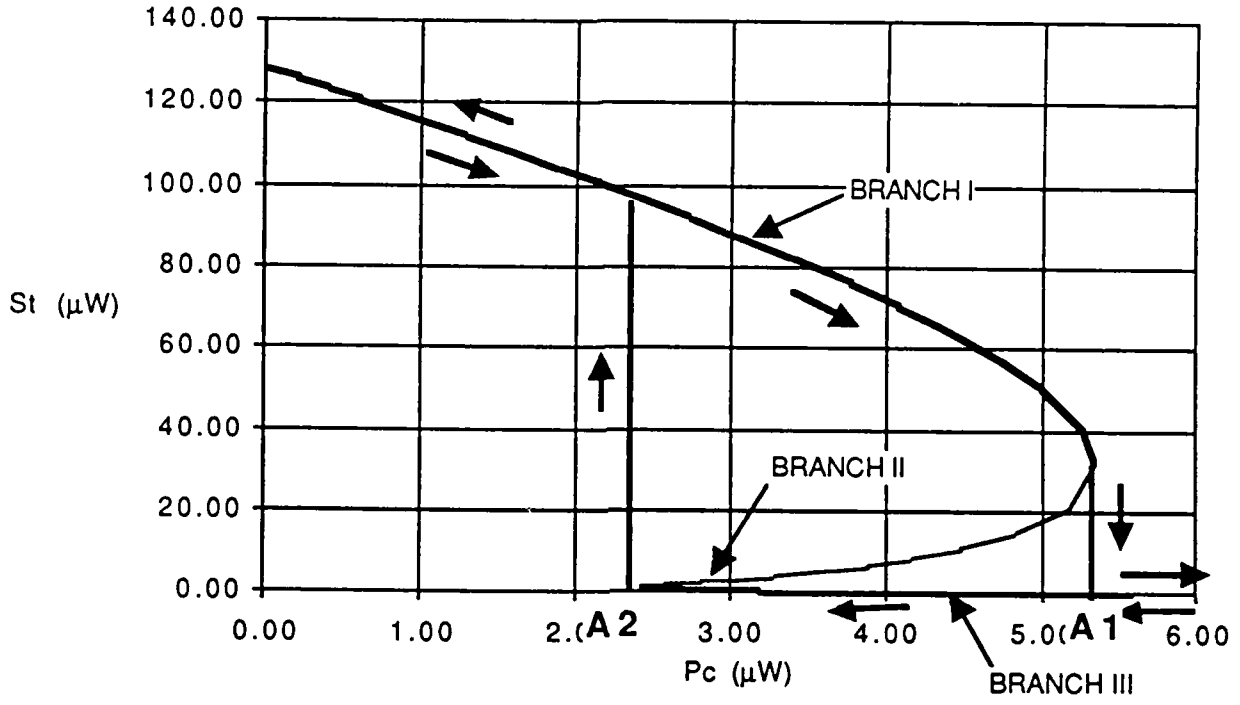

Figure 15. Hysteresis loop of bistable operation in class II operation.

either to the first branch or the third branch while entry into the second branch is prevented by the preexisting condition of excitation.

So far the discussion has been limited to phenomena derived on the basis of the steady-state rate equations. However, especially in bistable operation, some behavior of interest can occur when variables are changed at rates large compared to those of spontaneous emission or even of stored energy decay in etalons. Section 5.3 includes examples of that.

5.3 OPTIMIZED PARAMETER CHOICE FOR VARIOUS APPLICATIONS

5.3.1 QTE Switches

The memory action of Class II operation has certain advantages for high-speed switching of transmission and reflection with low power

expenditure. For example, the point at $P_c = 0$ on Branch I (see Figure 15) may be used for the transmission of a maximum signal, while at $P_c > A_1$ the signal S_t has a much lower value for the "off" position (with the corresponding inverse results for reflection).

The "off" position locates P_c in the region where the fluorescence parameter is dominant (Beer's Law) so that S_t has an $\exp(-cP_c)$ dependence in that region, where c is a parameter proportional to the 1→2 absorption cross section σ_{21}. It follows that S_t can be made arbitrarily small in the "off" position, albeit at the cost of (logarithmically) increasing control power P_c. If, on the other hand, P_c should be small, it is possible to reduce the power demand by a pulse method. To switch S_t from the "on" to the "off" condition, P_c is first pulsed to a value of $P_c > A_1$, then reduced to the lower value near A_2. Table 5, taken from a computer run similar to those reprinted in Tables 3 and 4, exemplifies the choice available for $S_0 = 128\ \mu W$, $R = 0.990$ in a sodium vapor etalon. As seen in Columns B, D, and E, P_c reaches a maximum (i.e., A_1) of about 18 μW. Thus, a pulse of $P_c =$ 20 μW, i.e., above A_1, for $\gamma_{12}^{-1} = 10$ ns duration transfers the QTE operation to Branch III, and subsequent relaxation of P_c to 3 μW maintains the operation at somewhat above $P_c = A_2$. Return to $P_c = 0$ reestablishes the original "on" position. This sequence switches the transmitted power from 128 μW to less than 0.01 μW and the reflected power from zero to almost 126 μW.

The pulse duration chosen corresponds to the spontaneous relaxation time, γ_{12}^{-1}, of sodium. However, considerably faster switching speeds are possible. If the same pump pulse energy is expended in 0.1 nsec with a peak power of $P_c = 2$ mW, the same switching action is obtained at hundred-fold speed. A similar gain in speed is obtainable for the transfer back to the "on"-position on Branch I. For this purpose, the value of P_c on Branch III after the 2 mW pulse has to be reduced to $P_c = 1.01\ A_2$. Then, when $P_c = 0$, the population in level 2 relaxes to the critical A_2 value in 1% of the spontaneous lifetime, i.e., switching to the upper branch occurs within $\simeq 0.1$ ns. It must be emphasized, however, that these short transit times apply only to the

Table 5

Sodium Vapor Etalon

	A	B	C	D	E	F	G	H	I
1	SIGNAL-	ABSORP-	MIROR	CONTROL	TRANSM.	RERLECTED	ABSORP		BEAM
2	INPUT	TION	REFLECT.	POWER	SIGNAL	SIGNAL	SIGNAL		MULT.
3	So (μW)	1-T	R	Pc (μW)	St(μW)	Sr (μW)	Sa(μW)	Sa/Pc	k
4	128.00	0.0000	0.990	0.0	128.00	0.00	0.00	#DIV/0!	199.00
5	128.00	0.0001	0.990	0.7	125.49	0.01	2.50	3.58	195.10
6	128.00	0.0002	0.990	1.4	123.05	0.05	4.90	3.58	191.31
7	128.00	0.0003	0.990	2.0	120.69	0.11	7.21	3.58	187.63
8	128.00	0.0005	0.990	3.2	116.15	0.29	11.56	3.58	180.58
9	128.00	0.0007	0.990	4.4	111.87	0.54	15.59	3.58	173.92
10	128.00	0.0009	0.990	5.4	107.82	0.87	19.32	3.58	167.62
11	128.00	0.0011	0.990	6.4	103.98	1.25	22.77	3.58	161.66
12	128.00	0.0013	0.990	7.3	100.34	1.68	25.98	3.58	156.00
13	128.00	0.0015	0.990	8.1	96.89	2.16	28.94	3.58	150.64
14	128.00	0.0018	0.990	9.2	92.04	2.96	33.00	3.58	143.10
15	128.00	0.0021	0.990	10.2	87.55	3.83	36.62	3.58	136.11
16	128.00	0.0025	0.990	11.4	82.04	5.09	40.87	3.58	127.55
17	128.00	0.0030	0.990	12.7	75.86	6.78	45.36	3.58	117.94
18	128.00	0.0035	0.990	13.7	70.35	8.56	49.09	3.58	109.37
19	128.00	0.0040	0.990	14.6	65.42	10.40	52.18	3.58	101.70
20	128.00	0.0050	0.990	15.9	56.98	14.17	56.84	3.58	88.59
21	128.00	0.0060	0.990	16.7	50.07	17.95	59.97	3.59	77.85
22	128.00	0.0080	0.990	17.6	39.54	25.26	63.20	3.59	61.47
23	128.00	0.0100	0.990	17.8	32.00	32.00	64.00	3.59	49.75
24	128.00	0.0150	0.990	17.1	20.42	46.17	61.41	3.60	31.74
25	128.00	0.0200	0.990	15.8	14.13	57.08	56.80	3.60	21.96
26	128.00	0.0250	0.990	14.5	10.33	65.59	52.08	3.60	16.07
27	128.00	0.0300	0.990	13.2	7.88	72.36	47.76	3.61	12.25
28	128.00	0.0350	0.990	12.2	6.20	77.86	43.94	3.61	9.63
29	128.00	0.0400	0.990	11.2	4.99	82.41	40.59	3.61	7.77
30	128.00	0.0500	0.990	9.7	3.43	89.49	35.08	3.61	5.34
31	128.00	0.0600	0.990	8.5	2.50	94.72	30.78	3.60	3.88
32	128.00	0.0700	0.990	7.6	1.89	98.74	27.37	3.59	2.94
33	128.00	0.0800	0.990	6.9	1.48	101.93	24.59	3.58	2.30
34	128.00	0.0900	0.990	6.3	1.19	104.52	22.30	3.57	1.84
35	128.00	0.1000	0.990	5.7	0.97	106.66	20.37	3.55	1.51
36	128.00	0.1200	0.990	5.0	0.68	110.00	17.33	3.50	1.06
37	128.00	0.1600	0.990	3.9	0.38	114.39	13.23	3.36	0.59
38	128.00	0.2000	0.990	3.3	0.24	117.16	10.60	3.18	0.37
39	128.00	0.2500	0.990	2.9	0.14	119.45	8.41	2.91	0.23
40	128.00	0.3000	0.990	2.6	0.10	121.01	6.90	2.61	0.15
41	128.00	0.3500	0.990	2.5	0.07	122.14	5.79	2.31	0.10
42	128.00	0.4000	0.990	2.4	0.05	123.00	4.95	2.03	0.07
43	128.00	0.5000	0.990	2.5	0.03	124.22	3.75	1.53	0.04
44	128.00	0.6000	0.990	2.6	0.01	125.05	2.94	1.14	0.02
45	128.00	0.7000	0.990	2.8	0.01	125.64	2.35	0.85	0.01
46	128.00	0.8000	0.990	3.0	0.00	126.09	1.91	0.64	0.01
47	128.00	0.9000	0.990	3.2	0.00	126.44	1.56	0.48	0.00
48	128.00	0.9500	0.990	3.4	0.00	126.59	1.41	0.42	0.00

transitions between Branches I and III. After a population N_2 in level 2 has been produced corresponding to $P_c > A_1$, it can relax to the value corresponding to $P_c = 1.01\ A_2$ only at the spontaneous emission rate γ_{12}. Thus, the system must remain on branch III for durations in the order of the radiative lifetime γ_{12}. This sets the frequency limit for such applications as multivibrators. Design optimization can improve the frequency limit by reducing the interval between A_1 and A_2 with a suitable parameter choice and other means.

5.3.2 QTE Transistors

Class II Operation. In principle, gains of almost any desired amount, $-dS_t/dP_c$ or dS_r/dP_c, respectively, for transmission or reflection, can be obtained on Branch I of Class II operation, as seen in Figure 13. It is only required that the control power and its maximum positive excursion, $P_c+\Delta P_c$, do not exceed the apex. In practice, fluctuations δP (i.e., noise) of the control power and the resulting instability of operation set a limit to the gain. Noise, of course, is always amplified along with signal. However, in the operation on Branch I near the apex, a fluctuation of $(P_c + \Delta P_c)$ by δP_c, which drives the control power beyond A_1, results in transition to Branch III. To the extent to which the range of fluctuations is known, the closest allowable approach of P_c to A_1 and the largest stable gain can be predicted. On statistical grounds, any fluctuation can be expected for a suffiently long observation time, so that the "maximum" fluctuation is that which is expected with a sufficiently high probability during the time of operation. For example, assume that the expected limit of $(\Delta P_c + \delta P_c)$ is not more than 2% of P_c. Table 4 is a computer printout of values varied in small amounts around the apex for an etalon with a lithium medium at $S_0 = 125\ \mu W$. The apex A_1 is reached for $P_c = 5.316\ \mu W$ so that the largest stable operating point of P_c is $5.210\ \mu W$. The allowable value of the gain is then about $dS_t/dP_c = -58$ for transmission and $dS_r/dP_c = 47$ for reflection.

Class I Operation. As described in Section 5.2, Class I operation (defined by Equation 5-10) is dominated by fluorescence through the entire range of the control power P_c. Therefore, transmission S_t and reflection S_r are univalued functions of P_c which each are described by a single branch. Thus, there exists no region of instability. This regime of operation, which is characterized by relatively small values of the incident signal power S_0, could of course be found by a somewhat extended search by computer. However, it is best to proceed first analytically since the slope characteristics of the two classes are markedly different. In particular the slopes of the branches in Class II have no real maximum amount since they vary at the apexes from $-\infty$ to $+\infty$ or vice versa. On the other hand, the slope of the single branch in Class I may have a minimum for S_t and a maximum for S_r where $S_t(P_c)$ and $S_r(P_c)$ have a point of inflection.

The minimum for the transmission gain, dS_t/dP_c, can be found by differentiating Equation 5-13 with respect to the single-pass absorption $\tau(=1 - T)$, which amounts to finding where the derivative of the denominator vanishes. One obtains for the (absolute value) maximum:

$$\tau = - \rho + [2/3 \ \rho S_0/S_h]^{1/2} \qquad (5\text{-}15)$$

By introducing Equation 5-15 back into 5-13, one finds the minimum (i.e., maximum negative) gain for various combinations of τ, ρ, S_0, and S_h:

$$(dS_t/dP_c)_{min} = (G_{sat}/2) \ [1/3(2/3 \ S_o/\rho S_h)^{1/2} - 1]^{-1} \qquad (5\text{-}16)$$

However, Equation 5-16 was derived from Equation 5-13 which has general validity for Class I and Class II operation. As pointed out before, in Class I operation S_0 is small enough (or the fluorescence parameter is large enough) so that the gains do not change sign and S_t, as well as S_r, are univalued functions of P_c. Thus, Equation 5-16 is limited to Class I operation, if

$$1/3(2/3S_0/\rho S_h)^{1/2} < 1 \qquad (5\text{-}17)$$

which ensures that the transmission gain S_t remains negative for all P_c.

The limit condition, written as

$$(S_0/\rho S_h)_{po} = 13.5 \qquad (5\text{-}18)$$

is the *point of overlap* between Class I and Class II operation.

Introduction of Equation 5-15 into Equation 5-16 yields the condition of minimum slope in terms of τ and ρ, viz:

$$(dS_t/dP_c)_{min} = \rho G_{sat}/2/3(\tau - 2\rho) \qquad (5\text{-}19)$$

Thus, the point of overlap is given by

$$\tau_{po} = 2\rho \qquad (5\text{-}20)$$

The implications of Equations 5-15 to 5-20 are now the following:

Consider first a choice of mirror reflectivity ρ, incident signal power S_t, and the (single pass) half-gain parameter S_h according to Equations 5-15 and 5-17 well below the point of overlap. Then, although the transmission gain, dS_t/dP_c, is a single-valued and rather flat function of P_c, one operates at a point of inflection, at maximum (negative) gain. Stability is very high, and the gain for excursions from the point of inflection is nearly constant.

Second, consider an approach to the point of overlap, given by Equations 5-18 and 5-20. The closer this approach, the larger is the absolute value of the gain. Excursions, ΔP_c, and fluctuations, δP_c, do not interfere with stability, but the gain falls off for larger excursions, i.e., amplification becomes increasingly nonlinear as condition 5-18 is approached.

Equations 5-15 to 5-20 guided the search for these domains of operation in the computer program. An example for Class I operation is shown in Figures 16 and 17 with Table 6 for an etalon with R = 0.990 reflecting mirrors and with sodium vapor (S_h = 12.6 μW, G_{sat} = 3.52) as QET medium. The analytical procedure just outlined predicted S = 1.6 μW as the most suitable operating point. Figure 16 presents the computer-derived dependence of S_t on the control power for S_0 = 1.60 μW. The behavior of S_t and the gain dS_t/P_c as functions of P_c with S_0 = 1.64 μW is presented in greater detail for the large gain values by Figure 14 from the data in Table 6. The peak gain, near 2200, requires very precise positioning of the control bias as the price of such high gain. Since the peak gain is a point of deflection, small variations ΔP_c of P_c experience nearly constant gain. Fluctuations δP_c of P_c, with frequencies not exceeding the bandwidth of the device, produce the same gain (as they would in any other amplifier), but they do not lead to an instability of operation. Because of the symmetry exhibited by the gains in transmission and reflection, as shown by Equations 5-13 and 5-14, the behavior of reflection is qualitatively the same, and quantitatively nearly the same, as that of transmission, except for the sign.

Table 6

Class I Operation in Sodium

1-T interval =		0.0001						
SIGNAL-	ABSORP	MIROR	CONTROL	TRANSN	∂ abs=	REFLECTED	ABS IN	BEAM
INPUT	TION	REFLECT	POWER	SIGNAL	DIFF GAIN	SIGNAL	ETALON	MULT.
So (μW)	1 - T	R	Pc (μW)	St(μW)	∂St/∂Pc	Sr (μW)	Sia(μW)	k
1.64	0.0175	0.990	0.276145	0.22	-173	0.67	0.76	26.19
1.64	0.0176	0.990	0.276157	0.21	-193	0.67	0.76	25.92
1.64	0.0178	0.990	0.276168	0.21	-216	0.67	0.75	25.66
1.64	0.0179	0.990	0.276177	0.21	-244	0.68	0.75	25.40
1.64	0.0181	0.990	0.276185	0.21	-278	0.68	0.75	25.14
1.64	0.0182	0.990	0.276192	0.21	-319	0.69	0.75	24.89
1.64	0.0183	0.990	0.276198	0.20	-368	0.69	0.75	24.64
1.64	0.0185	0.990	0.276203	0.20	-429	0.69	0.75	24.40
1.64	0.0186	0.990	0.276208	0.20	-506	0.70	0.74	24.16
1.64	0.0188	0.990	0.276211	0.20	-601	0.70	0.74	23.92
1.64	0.0189	0.990	0.276214	0.20	-722	0.70	0.74	23.68
1.64	0.0190	0.990	0.276217	0.19	-875	0.71	0.74	23.45
1.64	0.0192	0.990	0.276219	0.19	-1,066	0.71	0.74	23.23
1.64	0.0193	0.990	0.276220	0.19	-1,298	0.71	0.74	23.00
1.64	0.0195	0.990	0.276221	0.19	-1,563	0.72	0.73	22.78
1.64	0.0196	0.990	0.276222	0.19	-1,830	0.72	0.73	22.57
1.64	0.0197	0.990	0.276223	0.18	-2,038	0.72	0.73	22.35
1.64	0.0199	0.990	0.276224	0.18	-2,116	0.73	0.73	22.14
1.64	0.0200	0.990	0.276225	0.18	-2,031	0.73	0.73	21.93
1.64	0.0202	0.990	0.276226	0.18	-1,817	0.74	0.73	21.73
1.64	0.0203	0.990	0.276227	0.18	-1,547	0.74	0.72	21.52
1.64	0.0204	0.990	0.276228	0.18	-1,280	0.74	0.72	21.32
1.64	0.0206	0.990	0.276229	0.17	-1,048	0.75	0.72	21.13
1.64	0.0207	0.990	0.276231	0.17	-857	0.75	0.72	20.93
1.64	0.0209	0.990	0.276233	0.17	-705	0.75	0.72	20.74
1.64	0.0210	0.990	0.276236	0.17	-586	0.76	0.72	20.55
1.64	0.0211	0.990	0.276239	0.17	-491	0.76	0.71	20.36
1.64	0.0213	0.990	0.276242	0.17	-416	0.76	0.71	20.18
1.64	0.0214	0.990	0.276246	0.16	-355	0.76	0.71	20.00
1.64	0.0216	0.990	0.276250	0.16	-306	0.77	0.71	19.82
1.64	0.0217	0.990	0.276255	0.16	-266	0.77	0.71	19.64
1.64	0.0218	0.990	0.276261	0.16	-233	0.77	0.71	19.47
1.64	0.0220	0.990	0.276268	0.16	-206	0.78	0.70	19.29
1.64	0.0221	0.990	0.276275	0.16	-183	0.78	0.70	19.12
1.64	0.0223	0.990	0.276283	0.16	-164	0.78	0.70	18.96
1.64	0.0224	0.990	0.276292	0.15	-147	0.79	0.70	18.79
1.64	0.0225	0.990	0.276301	0.15	-133	0.79	0.70	18.63
1.64	0.0227	0.990	0.276312	0.15	-120	0.79	0.69	18.47
1.64	0.0228	0.990	0.276323	0.15	-109	0.80	0.69	18.31
1.64	0.0230	0.990	0.276336	0.15	-100	0.80	0.69	18.15

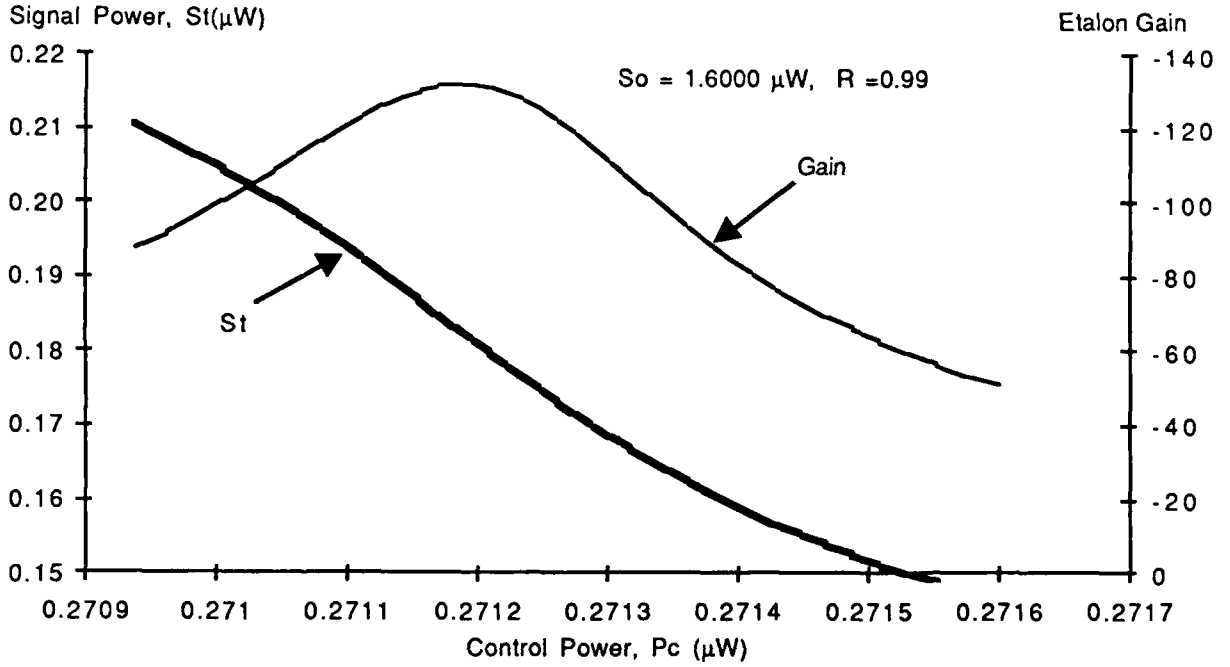

Figure 16. Class I operation in sodium.

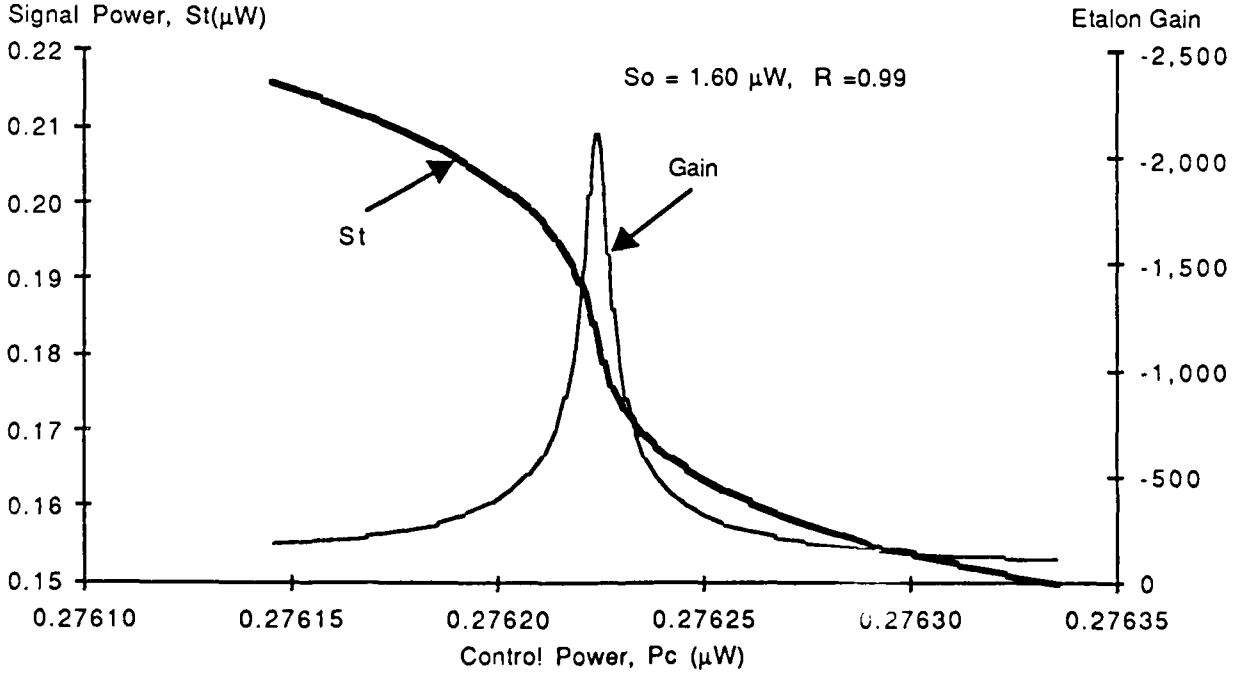

Figure 17. Detail of operation around maximum slop in sodium.

6. REFERENCES

1. Abraham and Smith, J. Phys. E.: Sci. Instrum., 33, 15 (1982).

2. A. M. Bonch-Bruevich, E. N. et al., Optics and Spectroscopy 27, 433 (1969).

3. T. A. Gould and T. Henningsen, "The Optical Switch and Transistor," Westinghouse Research Report 82-1F4-0TISC-R1 (Jan. 5, 1983).

4. I. N. Abramova, A. P. Abramov, and N. A. Tolstoi, Optics and Spectroscopy 27, 293 (1969).

5. See, e.g., A. Unsold, "Physik der Sternatmospheren," 2nd ed., Springer, Berlin (1955).

6. C. C. Corliss and W. R. Bozman, "Experimental Transition Probabilities for Spectral Lines of Seventy Elements," NBS Monograph 53 (1962).

7. See, e.g., E. O. Heavens, "Optical Properties of Thin Solid Films," Academic Press, New York (1955).

8. M. Garbuny, T. Henningsen, and R. H. Hopkins, "Program to Develop An Optical Transistor and Switch," Research Progress and Forecast Report for the period September 1, 1984 to March 30, 1985. Contract No. F49620-84-C-0103DEF, Air Force Office of Scientific Research.

9. Amnon Yariv, "Introduction to Optical Electronics," Holt (1971).

END

12-87

DTIC